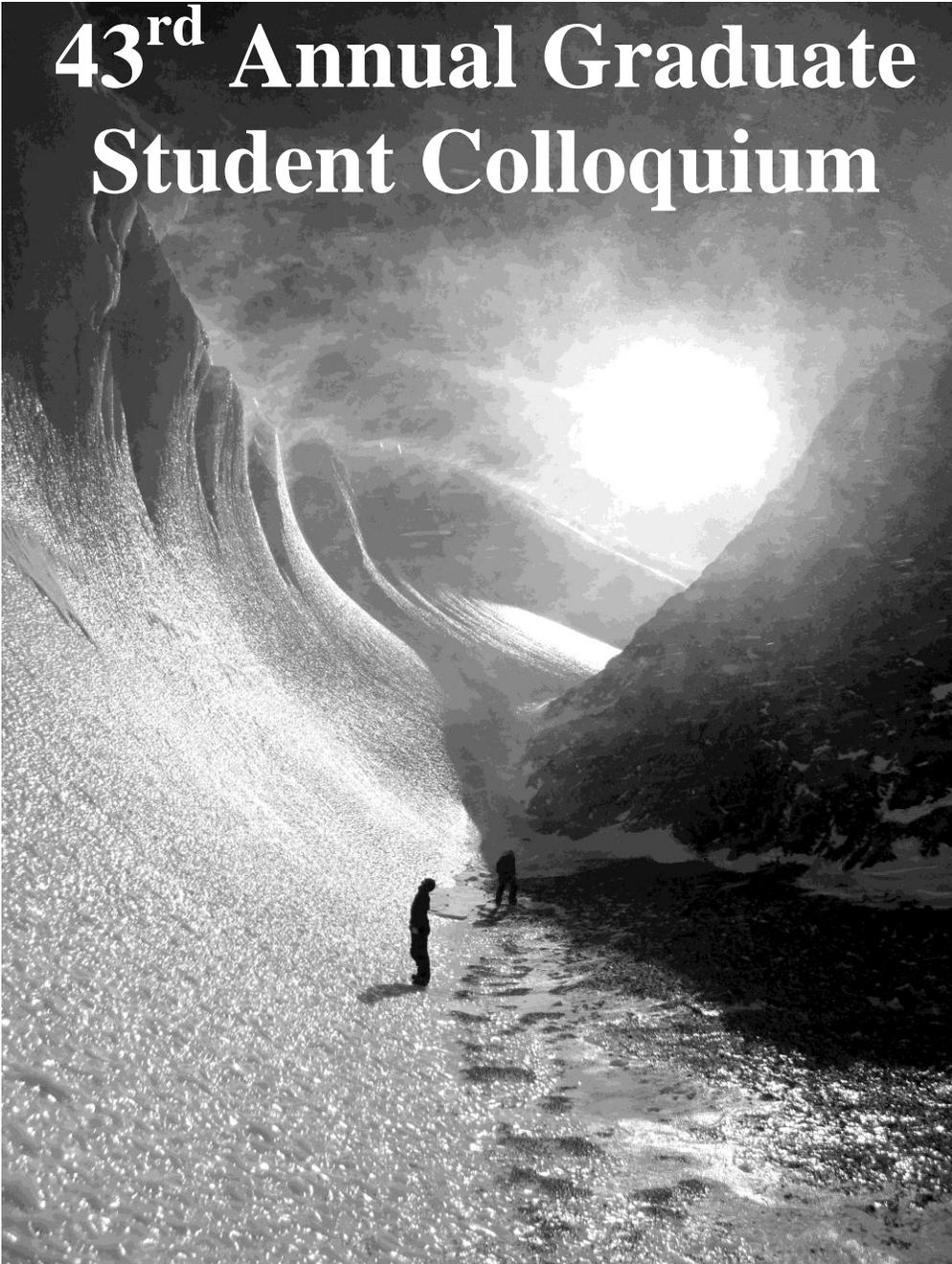# 43ʳᵈ Annual Graduate Student Colloquium

Windscoop, near Union Glacier Camp, Antarctica; photo by Lucas Zoet, 2010

Sponsored by Shell
Hosted by the Department of Geosciences

March 18-19, 2011

43rd Annual Graduate Student Colloquium

Sponsored by Shell and hosted by the Department of Geosciences
March 18-19, 2011

The Graduate Student Colloquium is a forum where students present their research or research proposal to faculty, friends, and peers. The Colloquium is hosted by the Department of Geosciences and is open to graduate students involved in geosciences research. The colloquium format stimulates research discussion, allows students to practice for national meetings, and helps students improve their presentation skills. The Colloquium assists both the Department and Penn State in maintaining and strengthening their reputations for giving high quality talks and poster presentations at national and international meetings.

The Graduate Colloquium Committee wishes to thank the students for sharing their work and the faculty for providing constructive feedback. The Committee also wishes to thank the Shell People Services division of Shell Oil Company for their generous financial support, and the Department of Geosciences for hosting this Colloquium.
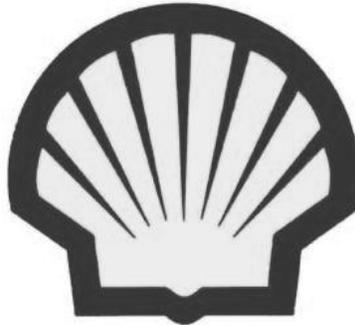
Schedule of Events

Event	Date and Time	Location
Poster Viewing	March 18, 6:30-8:30 March 19, 8:45-4:15	EES Atrium
Poster Session 1	March 18, 6:30-7:30	EES Atrium
Poster Session 2	March 18, 7:30-8:30	EES Atrium
Oral Session 1 – Mineralogy and Geochemistry	March 19, 8:45-10:00	114 EES
Break	March 19, 10:00-10:15	
Oral Session 2a – Biogeochemistry	March 19, 10:15-12:15	114 EES
Oral Session 2b – Petrology and Geodynamics	March 19, 10:15-12:15	116 EES
Lunch	March 19, 12:15-1:15	EES Atrium
Oral Session 3a – Ice and Climate	March 19, 1:15-2:45	114 EES
Oral Session 3b – Isotope geochemistry and Hydrogeology	March 19, 1:15-2:45	116 EES
Break	March 19, 2:45-3:00	
Oral Session 4 – Geobiology	March 19, 3:00-4:15	114 EES
Dinner and Discussion at the Marone's	March 19, 6:30 pm	591 E. Shadow Lane, State College

Graduate Student Colloquium
Committee Members
2011

Claire Fleeger, chair

Jamie Brainard
Monica Carvalho
Randy Justin
Lauren Milideo
Eriks Perkons
Kristina Peterson
Megan Pickard

The Peter Deines Lectureship

The first place award for an oral presentation by a post-comprehensive Ph.D. student is designated the Peter Deines Lectureship for the following academic year.

This award was started in 2004 to represent the tremendous amount of respect and admiration the graduate students in the Department of Geosciences had for Dr. Peter Deines, who that year was stepping down from the position of Graduate Program Chairman. Recipients of the honor are invited to give a departmental colloquium talk during the proceeding academic year.

The department and the world lost a great man and wonderful person when Peter passed away on February 2, 2009. It is with great pride that the Graduate Student Colloquium continues the tradition born in 2004.

Past Recipients:

2010-2011: Tim Fischer
2009-2010: Aaron Diefendorf and Bryn Kimball
2008-09: Daniel Hummer
2007-08: Gavin Hayes
2006-07: Christina Lopano
2005-06: Shawn Goldman and Courtney Turich
2004-05: Margaret Benoit

The Peter Deines Lectureship

Peter Deines (4/02/36 - 2/02/09) earned a Geologen Vordiplom at the Rheinsche Friedrich Wilhelms Universitaet, Bonn, Germany in 1959, an M.S. (1964) and a Ph.D. (1967) in Geochemistry and Mineralogy from Penn State University. Since 1967, and after 2004, as an Emeritus Professor, he was a member of the Geological Science Faculty of the Pennsylvania State University. He earned an international reputation for his geochemical research, teaching, and science administration. Recognition came in teaching awards, election to the University Senate, in which he served for 24 years, and election especially to Treasurer of the International Geochemical Society. In that office, he was so effective that he was awarded a unique Honorary Life Membership for his financial management of the society. He was a principal organizer of that Society's primary international meetings, the famous Goldschmidt Conferences.

With his gift for organization, he also served the Department of Geosciences on most of its committees and he served as its Graduate Program Chairman, while also administering committees for the College of Earth and Mineral Sciences, primarily for Scholarships. Most important was his commitment to the University Academic Senate, in which he served in 28 committee posts, including its Chair for 1990-91; and to the University, on 34 committees and commissions, including University Ombudsman since 2006. He also was elected President of the Faculty-Staff Club. Dr. Deines' research centered on precise explanations of natural variations in stable isotope abundances as means of understanding geologic processes. Results were presented in lectures throughout the world and in over 60 published papers. His illustrated book, "Solved Problems in Geochemistry," was polished by his teaching of eight graduate courses and is available on the web especially for graduate students.

A 40-year member of the Nittany Valley Symphony, Peter will be missed for his finesse with violin and viola.

Poster Session One

Friday, March 18
6:30-7:30 pm, EES Atrium

Poster #	Presenter	Advisor	Title
1	Victoria Miller	Barry Voight and Charles Ammon	Seismic expression of magma-induced crustal strains and localized fluid pressures during initial eruptive stages, Soufrière Hills volcano, Montserrat
3	Alison Sacks	Demian Saffer and Don Fisher	Stress and strain axes in the Kumano forearc basin from inversion of fault populations mapped in a 3D seismic volume, Nankai Trough, SE Japan
5	Elizabeth Desser	Andy Nyblade	Anisotropy in the western branch of the East African Rift System – New shear-wave splitting results
7	Jessica Yakob	Maureen Feineman	An Experimental Study of Li Partitioning Between Olivine and Diopside at Mantle Conditions
9	Katelyn Gerecht	Kamini Singha	Hyporheic Flow and Heat Transport Within a Bed-to-Bank Transect of a Large Regulated River: Colorado River, Austin, TX
11	James Deane	Maureen Feineman	Diffusion Induced Lithium Isotope Fractionation in Diopside
13	Andrew Lloyd	Andy Nyblade	Upper Mantle Structure Beneath the Gamburtsev Subglacial Mountains, East Antarctica via Body-Wave Tomography
15	Matthew Herman	Kevin Furlong	A Comparison of the Transpressional Boundaries in New Guinea and New Zealand
17	Jon Schueth	Tim Bralower	Calcareous nannoplankton and rapid climate change: Was high climate variability responsible for nannofloral turnover during the PETM and Plio-Pleistocene?
19	K. Michael Cleveland	Charles Ammon	Interacting Earthquakes Along the Northern Vanuatu Subduction Zone
21	Kristin Morell	Donald Fisher	Volcanic, exhumational and landscape response to late Miocene to recent plate tectonics, Central American Volcanic Arc
23	Gabriel Mulibo	Andrew Nyblade	Upper Mantle Structure of the Eastern Africa from Body Wave Tomography
25	Alysa Young	Andrew Nyblade	The Structure and Geology of Tanzanian Coastal Basins from P- and S-wave Receiver Functions

Seismic expression of magma-induced crustal strains and localized fluid pressures during initial eruptive stages, Soufrière Hills volcano, Montserrat

Victoria Miller
Ph.D. Student, Post-comps

Advisors: Barry Voight and Charles Ammon

Eylon Shalev, Institute of Earth Science and Engineering, University of Auckland
Glen Thompson, Geophysical Institute, University of Alaska Fairbanks

The andesite stratovolcano of Soufrière Hills, Montserrat, has been intermittently erupting since 1995. Eruption onset seismicity (July – August 1995) extended to depths >5 km whereas more recent seismicity has been confined to the upper 4 km. Here we explore volcanotectonic earthquake activity during the early stages of volcanic activity at Soufrière Hills volcano. This early seismicity, recorded over a broad region in south Montserrat, gives the seismic expression of magma ascent after decades of quiescence, and has an interesting distribution of clustered seismicity. We seek to improve understanding of this seismicity in relation to structures, heterogeneous media, and magma transport dynamics with associated force and fluid pore-pressure redistributions. We focus on several zones of temporally-confined seismic activity examining the seismicity in relation to regional tectonics and heterogeneity of stiffness and strength as revealed by the SEA-CALIPSO tomography experiment. The clustered seismicity and relatively aseismic zones are interpreted to reflect a broad weakened tectonic zone of ESE trend that crosses Montserrat, and the ascent of a magmatic dike of NNE trend, which altered the stress distribution to promote localized fault movements and caused localized dilatation with changes in pore-fluid pressures, to either weaken or strengthen the rock mass depending on the local strain.

Stress and strain axes in the Kumano forearc basin from inversion of fault populations mapped in a 3D seismic volume, Nankai Trough, SE Japan

Alison Sacks
M.S. Student

Advisor: Demian Saffer and Don Fisher

IODP drilling (part of NanTroSEIZE) at the Nankai Trough off Kii Peninsula documented an abrupt change in the orientation of maximum horizontal stress across a major out-of-sequence-thrust fault (OOST). This fault extends >120 km along strike and forms the seaward boundary of the Kumano forearc basin. Borehole breakouts indicate that the orientation of maximum horizontal stress changes from 150/330 in the prism to 044/224 in the forearc basin across the OOST, just 10 km landward. A borehole 15 km further landward in the forearc basin indicates an orientation of 150/330. Analysis of a 3D seismic volume defines a population of normal faults within recent (0-3.8 Ma) Kumano forearc basin strata, which we used to infer current and historical strains and stresses. Normal faults are generally restricted to the gently dipping cover sequence that unconformably overlies the older (late Miocene) accretionary prism. Using cross-cutting relationships and sea-floor scarps, we divided the population into three chronological sub-groups. The oldest group consists of SE-NW striking faults which are always cross-cut. The remaining faults, all approximately E-W striking, are classified as intermediate in age if they do not exhibit a scarp the sea floor, and as youngest if a scarp is present. All inversions were performed using T-TECTO 3.0, software created by Jure Žalohar and Marko Vrabec. Assuming that motion along faults is purely dip-slip, using Molnar's method we found that the maximum extension direction varies between 030/210 and 080/260 for the oldest faults. Both the youngest and intermediate aged populations produce a consistent maximum extension direction of ~170/350, nearly parallel to the direction of plate convergence and the shortening direction inferred for the outer accretionary wedge near the trench. Inversion for principal stress orientations (Angelier 1984) yielded a vertical maximum principal stress and sub-horizontal intermediate and minimum principal stresses for all age groups. The minimum principal stress is oriented ~ NE for the oldest faults, while the intermediate and youngest populations indicate equal magnitudes of intermediate and minimum stress throughout the basin. The principal axes of strain and stress determined from inversion of the youngest faults are generally consistent with stresses inferred from borehole breakouts at the two boreholes in the basin. Several mechanisms have been proposed to drive the extension observed in forearc wedges. In the Nankai subduction zone, this extension may be attributed to prevailing stress conditions within the accretionary wedge, a response to gravitational stresses within the shallow sediments, or tilting of the basin related to slip on the megasplay fault.

Anisotropy in the western branch of the East African Rift System – New shear-wave splitting results

Elizabeth Desser
M.S. Student

Advisor: Andy Nyblade

Angela Reusch, IRIS PASSCAL Instrument Center, Socorro, New Mexico
Aubreya Adams, Chevron Corp., Covington, Louisiana
Gabriel Mulibo, Department of Geosciences, Penn State
Fred A. Tugume, Department of Geosciences, Penn State
Winchelle Sevilla, Department of Geosciences, Penn State
Richard Ferdinand, University of Dar es Salaam, United Republic of Tanzania

To advance our understanding of the formation and evolution of the East African Rift System (EARS), we use new shear-wave splitting results to characterize the seismic anisotropy of the upper mantle along the western edge of the Tanzania Craton, and the western branch of the EAR. Results from previous studies of shear-wave splitting in East Africa suggest multiple sources of anisotropy in the EAR, such as asthenospheric flow around the Tanzania Craton lithosphere, mantle plume perturbations, fossil anisotropy associated with paleo-orogenic systems, and magma lenses with fast directions parallel to the rift. We employ the shear-wave splitting processing program, SplitLab, to measure the apparent splitting of teleseismic shear wave phases recorded on 40 broadband seismic stations deployed in Uganda and Tanzania from 2007 to 2010. Our results will be compared with previous studies in the EAR, along with those from other world rift systems, to further evaluate the causes of anisotropy in the East African mantle.

An Experimental Study of Li Partitioning Between Olivine and Diopside at Mantle Conditions

Jessica L. Yakob
M.S. Student

Advisor: Maureen D. Feineman

Sarah C. Penniston-Dorland, University of Maryland
David H. Eggler, Penn State University

Measured ^{7}Li/^{6}Li of mineral separates from mantle xenoliths from diverse localities show unexpectedly large differences between olivines and pyroxenes, often with lighter Li found in the pyroxenes (Jeffcoate *et al.*, 2007; Rudnick and Ionov, 2007; Ionov and Seitz, 2008). Although changes in isotopic fractionation with temperature could explain the differences, a kinetic isotope effect is as likely. Because ^{6}Li diffuses faster than ^{7}Li, bulk lithium exchange between two phases could result in dynamic isotopic fractionation, with the receiving phase becoming lighter and the donating phase becoming heavier. Thus if Li becomes more compatible in cpx upon cooling, that is, if $D_{Li}^{ol/cpx}$ is temperature-dependent, the diffusive exchange of Li will generate temporary ^{6}Li enrichment in cpx and depletion in olivine. Experiments were conducted using a piston cylinder apparatus at 1100°C and 1.4 GPa (1-5 days) to determine $D_{Li}^{ol/cpx}$. San Carlos olivine and Dekalb diopside were finely ground for starting materials. A mixture of olivine (52 wt%), diopside (34 wt%), albite (7 wt%), and quartz (7 wt%) powders (0.0145 g) was loaded into a Pt capsule inside of a Ni crucible. Milli-Q water with 100 ppm Li and 500 ppm Ba (obtained through dilution of stock solutions) was added (0.1100 g) to serve as the lithium source. Lithium concentrations in olivine and diopside from experiments held for 1, 3, and 5 days were determined by laser ablation ICP-MS. Partition coefficients $D_{Li}^{ol/cpx}$ from runs at 3 and 5 days are, within error, the same, 2.2 (0.1). These fall in the lower portion of the range, D = 2-7, of limited previous measurements (Brenan *et al.*, 1998b, Blundy and Dalton, 2000; Caciagli-Warman 2010).

Hyporheic Flow and Heat Transport Within a Bed-to-Bank Transect of a Large Regulated River: Colorado River, Austin, TX

Katy Gerecht
Ph.D. Student, Pre-Comps

Advisor: Kamini Singha

M. Bayani Cardenas, Jackson School of Geosciences, University of Texas at Austin
Andrew J. Guswa, Picker Engineering Program, Smith College
Audrey H. Sawyer, Jackson School of Geosciences, University of Texas at Austin
Travis Swanson, Jackson School of Geosciences, University of Texas at Austin
John D. Nowinski, Jackson School of Geosciences, University of Texas at Austin

The stage and discharge of the Lower Colorado River (LCR) near Austin, Texas is regulated by a series of dams for hydropower generation, flood management, water supply, and recreation. Daily releases from a dam, 23 km upstream of the study site, cause the stage at the site to fluctuate by more than 1.5 m with a mean depth of 1.3 m. These fluctuations cause the LCR at the study site to transition from a regionally gaining river to a river that both gains and loses over each daily cycle. To assess the effects of the flow management on river-groundwater exchange, we collected temperature and head measurements across a hyporheic-to-riparian transect that were highly resolved in both space and time over two campaigns of three days each. These observations show that river-groundwater exchange flux is consistently larger close to the bank and decreases with distance from the bank. Correspondingly, both the depth of the hyporheic zone and the exchange time are greatest near the bank. Adjacent to the bank streambed head response is hysteretic, with hysteresis dissipating with increased distance from the bank, indicating that transient bank storage affects the direction and magnitude of vertical exchange close to the bank. Hyporheic zone temperature is perturbed up to one meter below the bed. When the river stage is high, which coincides with when the river is coldest, downward advection of heat from a previous cycles' warm-water pulse warms the hyporheic zone. When the river is at its lowest stage but warmest temperature, upwelling groundwater cools the hyporheic zone. These hydraulic and thermal alterations may change the biogeochemical and ecologic dynamics of the river and its hyporheic and riparian zones, including the hyporheic zone's capacity to act as a biological filter and habitat.

Diffusion Induced Lithium Isotope Fractionation in Diopside

James A. Deane Jr.
M.S. Student

Advisor: Maureen Feineman

Lithium has been shown to be a fluid mobile element with a high diffusion coefficient compared to other cations (Coogan et al. 2005). Richter et al. (2003) showed lithium isotopically fractionates up to 40 ‰ during diffusion due to the rapid diffusion of ^{6}Li relative to ^{7}Li. Lithium has a broad range of isotopic ratios in natural materials at the Earth's surface; for example seawater has a distinct δLi^7 of ~32‰ and unaltered oceanic crust has a δLi^7 of ~4‰ (Tomascak 2004). Knowing these values and how Li interacts with rocks and fluids under temperature and pressure conditions relevant to the mantle, we can better describe how subduction processes work by looking at Li signals in volcanic settings. With better experimental constraints on Li partition coefficients, diffusion coefficients, and isotopic fractionation factors, Li in mantle minerals could be used as a tracer for fluid rock interactions in subduction zones, and as a geospeedometer to track rates of magmatic processes. To measure the diffusion rates and isotopic fractionation of Li caused by diffusion in diopside, a slab was cut and polished perpendicular to the *c*-axis of the crystal, surrounded by a Li enriched source, and left held at 10 kbar and 900°C for 48 hours in a piston cylinder apparatus. The resulting diffusion profiles can be measured by laser ablation inductively coupled plasma mass spectrometry (LA-ICP-MS) and values for the diffusion coefficient will be determined. In addition, Li isotope ratios will be determined by secondary ionization mass spectrometry (SIMS) to determine the extent of isotopic fractionation during diffusion. To obtain meaningful experimental results, the diopside used as a starting material must be homogeneous with respect to major element composition, Li concentrations, and Li isotope ratios. Initial Li concentrations were determined to be 35±5ppm by electron probe microanalysis (EPMA) and LA-ICP-MS at the University of Maryland.

Coogan Laurence A., Kasemann Simone A., Chakraborty Sumit. "Rates of hydrothermal cooling   of new oceanic upper crust derived from lithium-geospeedometry." Earth and Planetary Science Letters 240, 2005

Richter Frank M., Davis Andrew M., DePaolo Donald J., Watson Bruce E. "Isotope   fractionation by chemical diffusion between molten basalt and rhyolite." Geochemica et   Cosmochemica Acta Vol. 67, No. 20, pp. 3905-3923. 2003

Tomascak Paul B. "Developments in the Understanding and Application of Lithium Isotopes   in the Earth and Planetary Sciences." Reviews in Mineralogy & Geochemistry Vol. 55,   pp. 153-195, 2004

Upper Mantle Structure Beneath the Gamburtsev Subglacial Mountains, East Antarctica via Body-Wave Tomography

Andrew Lloyd
M.S. Student

Advisor: Andy Nyblade

Doug Wiens, Washington University in St. Louis
Sam Hansen, University of Alabama

The geophysical mechanism responsible for the uplift of the Gamburtsev Subglacial Mountains is poorly understood. Many uplift models for the region have been invoked, such as the existence of a hotspot or a series of Proterozoic/early Paleozoic orogenic events. Past seismic studies have been limited to continental scale surface wave tomography with spatial resolution no better than 600 km, leaving the Gamburtsev Mountains relatively unexplored. Using seismic data from the GAMSEIS array we investigate the geologic structure of this unique subglacial mountain range. The GAMSEIS array consisted of 26 temporary broadband stations, 12 stations were arranged in a linear array as a continuation of the TAMSEIS array, 6 stations were arranged in a second linear array intersecting the first array, and 8 stations were install between the two linear arrays to improve 3-D resolution. Here we investigate the upper mantle structure via regional body-wave tomography using P & S travel times from teleseismic events. Geometric crust and ice effects, determined by receiver functions, are removed when calculating the relative travel time residuals. Preliminary P velocity models using 3892 ray paths from 288 teleseismic events indicate velocity perturbations between +/- 0.5%, likely ruling out any uplift models that require the presence of a thermal anomaly beneath the Gamburtsev Mountains.

A Comparison of the Transpressional Boundaries in New Guinea and New Zealand

Matthew Herman
M.S. Student

Advisor: Kevin Furlong

Harley Benz, National Earthquake Information Center, USGS
Gavin Hayes, National Earthquake Information Center, USGS

Mountain ranges that develop along transpressive plate boundaries tend to be narrow, but can have very rapid rates of uplift. The Highlands fold and thrust belt is such a transpressive orogen, extending ~2000 km along the spine of New Guinea. The belt undergoes rapid uplift as part of the left lateral transpressive collision between the Australia plate continental margin and elements of the Pacific plate to the north. Regional Australia-Pacific plate motions over the past 5-8 Ma average 110 mm/yr at an orientation of N60°E and the structures of the mountain belt trend nearly east-west, thus the angle between Australia-Pacific relative velocity and the diffuse plate boundary through New Guinea is approximately 30°. We compare the Highlands fold and thrust belt to the Alpine Fault and Southern Alps transpressive orogen. There are differences in rate and scale between the two locations: the Southern Alps are a smaller mountain range, extending ~600 km across the South Island of New Zealand, and the Australia-Pacific plate velocity is only 35 mm/yr. However, there are also several similarities between the two plate boundary segments, which allow us to compare them. Both are characterized by similarly narrow mountain ranges and convergence obliquity, both reflect portions of a more extensive transpressive plate boundary with the orogen developing along the segment between continental blocks, and both have experienced rapid changes in plate boundary orientation and style in the past 25 Ma. Simple comparisons of the deformation rate (as measured by total moment released in 50 years per unit area) and elevation profiles of the mountain ranges suggest that the difference in plate velocity may be the dominant kinematic factor controlling the variations in the physical characteristics of these orogens. As expected, the New Guinea orogen experienced approximately three times the deformation rate and had a cross section that was three times greater, but it is still uncertain why the orogen grew significantly taller but not wider than the New Zealand orogen.

Calcareous nannoplankton and rapid climate change: Was high climate variability responsible for nannofloral turnover during the PETM and Plio-Pleistocene?

Jon Schueth
Ph.D. Student, Pre-comps

Advisor: Tim Bralower

Modern climate change can drastically alter oceanic ecosystems and cause vast community disruptions and extinctions. However, the long-term effects of such drastic change are not known. Rapid climate change can push life to the limits of ecosystem tolerances, making extinction more likely. One of the best ways to understand long-term planktonic ecosystem responses is to study how previous climate changes impacted plankton assemblages. Calcareous nannoplankton are a good target for such an investigation because most species have very specific temperature and nutrient tolerances, and the group has a highly detailed fossil record. Most notably, there are two primary nannoplankton turnover events tied closely to significant climate changes, the rapid warming associated with the Paleocene-Eocene Thermal Maximum (PETM) and global cooling and enhanced glaciations in the northern hemisphere in the Pliocene and Pleistocene. These nannoplankton turnovers were likely a result of rapid niche space shifts caused by high rates of change in key environmental variables such as temperature and nutrients. Because rates are usually calculated as the change between data points, they may not represent true paleoecologic processes. To obtain a more accurate representation of past rates of change, rate models were constructed by applying paleoecological data from Ocean Drilling Program sites using statistical techniques common in modern ecological studies. These techniques have not been extensively applied to paleoecological problems. Nannoplankton abundance is most variable when the environmental rate of change is the highest, and some taxa go extinct while environmental variability is high or slightly after a period of rapid climate change. Several taxa that are dominant or have a wide geographical range are less variable during rapid change, suggesting that these characteristics may lower the probability of extinction during rapid ecospace shifts. These results show that community changes and turnover are more likely when the rate of climate change is high. Therefore it seems likely that if modern anthropogenic climate change continues at such a rapid pace, marine planktonic ecosystems could experience major turnover in the future.

Interacting Earthquakes Along the Northern Vanuatu Subduction Zone

Michael Cleveland
M.S. Student

Advisor: Charles J. Ammon

Thorne Lay, University of California, Santa Cruz

Located in the southwest Pacific, the Vanuatu subduction zone displays diverse seismic behavior, characterized by frequent moderately sized earthquakes (Mw 5-7), but relatively few events larger than Mw 7.0. The seismic character also varies regionally along the length of the trench. On 07 October 2009 the northern segment of the Vanuatu subduction zone (11° to 14°S) ruptured in three large, shallow, thrust earthquakes. All three (Mw 7.7, 7.8, and 7.4) occurred in close proximity and over the duration of about one hour. Historical seismicity shows this region of the trench has experienced multiple shallow, large (Mw >7.0), thrust events during the past century, including large shallow doublets in 1966 and 1980. The July 1980 earthquake doublet (Mw 7.5, 7.7) ruptured the plate boundary in approximately the same location as the 2009 sequence. The focal mechanisms of these earlier events are similar to one another and to the mechanisms of the 2009 events. The close spatial proximity and similarity in focal mechanisms of these earthquake sequences suggests this portion of the subduction zone may fail in characteristic multiplet earthquakes. Large, shallow, thrust earthquakes have been observed to occur in pairs and multiples in various tectonic regimes, but there are no unifying tectonic characteristic producing these sequences. We present rupture models for the larger events in the region (for which teleseismic body waves can be isolated), and explore the relative locations of the 2009 events and earlier events using regional and teleseismic surface waves. Our goal is to map the region of the plate boundaries failing in the large multiplets of the region in hopes of understanding the spatial and temporal relationships between these potentially interacting earthquakes.

Volcanic, exhumational and landscape response to late Miocene to recent plate tectonics, Central American Volcanic Arc

Kristin Morell
Ph.D. Student, Post-comps

Advisor: Donald Fisher

Eric Kirby, Penn State

New analysis of the rates and patterns of incision, uplift and erosion within the Central American volcanic arc indicate a marked landscape response to uplift produced by low-angle subduction of the ~20 km thick Cocos Ridge. We focus on the Talamancas Range, the now-extinct and highly exhumed Miocene arc located directly inboard of the Cocos Ridge in Central Costa Rica. The range is highly asymmetric in cross-section, with the highest relief and steepest rivers occurring south of the divide. In the area north of the divide we identify a transient landscape, recognized by a perched low-relief surface at high elevations, that also coincides with the location of ~25 knickpoints. Each knickpoint separates a gently sloping upstream channel segment from a steeper downstream reach. Knickpoints cluster around a constant elevation, do not coincide with major lithologic boundaries, and occur below the ice extent associated with the last glacial maximum. By reconstructing the paleo-tributary networks of the low-relief surface, we estimate ~2 km of rock uplift since the onset of increased incision. We suggest that both the high relief observed in the southern flanks, and the increased incision recorded by the transient are produced by increased rock uplift caused by subduction of the Cocos Ridge. These results are consistent with plate reconstruction models which predict an early arrival of the Cocos ridge at the subduction zone of ~3 Ma. Comparison of this result to radiometric ages from both the Panamaian and Costa Rican extinct arcs suggests that extinction of arc volcanism within both these ranges could be due to changing plate tectonics during the late Miocene, and may not be related to Cocos Ridge collision.

Upper Mantle Structure of the Eastern Africa from Body Wave Tomography

Gabriel Mulibo
Ph.D. student, Post-comps

Advisor: Andrew A. Nyblade

R.W. Ferdinand, University of Dar es Salaam, Tanzania

This study presents preliminary results of the upper mantle structure beneath the east Africa from body wave tomography. This work is part of an on-going study aimed at investigating the origin and structure of the African Superplume. The available global tomographic studies suggest that the African Superplume is a low velocity-anomaly extending from the core-mantle boundary upward into the mid mantle beneath southern Africa and may reach the upper mantle beneath eastern Africa. However, the limited vertical resolution of global tomographic models makes it difficult to confirm a connection from the lower to the upper mantle. Previous regional studies of upper mantle structure in east Africa have found evidence of a low velocity anomaly beneath the region that has been suggested as the upper mantle expression of the Superplume. Models from previous tomographic studies in east Africa have limited resolution below ~400 km beneath the eastern rift and are less well resolved beneath the western part of the rift due to less data coverage. This study uses teleseismic data from a wider region in east Africa than previously used.

Data for this study are from a 3-year (2007-2010) deployment of 40 broadband seismic stations in Uganda and Tanzania. The dataset is supplemented by data from the 1994-1995 Tanzania broadband seismic experiment, the 2001-2002 Kenya broadband seismic experiment, the permanent AfricaArray seismic stations and IRIS/GSN stations. The data have been used for body wave tomography by computing relative travel time delays using a multi-channel cross-correlation technique and then inverting them for a 3D wave speed model. Preliminary results from the inversion of the relative delay times show that there is a broad low wave speed anomaly beneath east Africa extending from shallow upper mantle depths to at least 500 km into the mantle transition zone. The appearance and size of the low wave speed anomaly in the region indicates the presence of broad thermal anomaly associated with the African Superplume.

The Structure and Geology of Tanzanian Coastal Basins from P- and S-wave Receiver Functions

Alysa Young
M.S. Student

Advisor: Andrew Nyblade

The structure of Jurassic to Neogene coastal basins along the Tanzania passive margin and crustal thickness beneath them are being investigated in this study using P- and S-wave receiver functions. Seismic data recorded by eight stations deployed from February 2010 through today provide the primary dataset. Receiver functions have been computed using ~200 teleseismic events. The resulting waveforms, consisting of several Ps arrivals in the first 5s, indicate complicated crustal structure. To estimate crustal thickness, the h-k stacking method was used for each station. Well-resolved results from one station yield crustal thickness of approximately 40km, with an average Vp/Vs of 1.64. To estimate basin thickness, the Ps arrival times from the sediment-rock interface and its multiples have been combined with assumed Vp/Vs ratios for shales and sandstone. Basin thicknesses of between 2 and 6km were obtained. Future work will consist of the computation of S-wave receiver functions, synthetics, and joint inversions. Results from each approach will, together, provide the best estimate of basin and crustal structure for this region.

Poster Session Two

Friday, March 18
7:30-8:30 pm, EES Atrium

Poster #	Presenter	Advisor	Title
2	Marco Maria Scuderi	Chris Marone	Mapping the brittle-ductile transition in shales
4	Daniel Kohl	Rudy Slingerland	Sequence Stratigraphic Analysis of the Marcellus Shale and Associated Strata
6	Brett Carpenter	Chris Marone and Demian Saffer	Frictional and hydrologic behavior of the San Andreas Fault: Insights from laboratory experiments on SAFOD cuttings and core
8	Xuhua Shi	Eric Kirby	Abrupt lake level rise of the Siling Co (Lake) in recent ten years, induced by glacial melting in central Tibetan Plateau
10	Megan Carter	Susan Brantley	The effect of Giant Sequoia trees on mineral weathering
12	Matthew Gonzales	Matthew Fantle	Solution composition-dependence of the Ca isotope composition of inorganic calcite
14	Alex Burpee	Rudy Slingerland	The Role of Grain Caliber in Determining Delta Morphology
16	Russell Rosenberg	Eric Kirby	$^{40}Ar/^{39}Ar$ Dating of Basalt Flows Capping the Tertiary Brown's Park Formation Provide New Constraints on the Neogene Incision and Uplift History of the Yampa and Little Snake Rivers, Colorado
18	Hiroshi Hamasaki	Hiroshi Ohmoto	An experimental investigation of multiple sulfur isotope fractionations during heterogeneous reactions between SO2 and activated carbon
20	Lucas Zoet	Sridhar Anandakrishnan	Laboratory Observations of Ice's Deformational Properties
22	Fred Tugume	Andrew Nyblade	The crustal structure of East Africa
24	Tim Murray	Maureen Feineman	Understanding arc magma evolution in thick continental crust

Mapping the brittle-ductile transition in shales

Marco Maria Scuderi
Ph.D. Student, Pre-comps, Petroleum related

Advisor: Chris Marone

B. M. Carpenter, Department of geosciences, Pennsylvania State University
D. Elsworth, Department of geosciences, Pennsylvania State University
D. M. Saffer, Department of geosciences, Pennsylvania State University
Hiroko Kitajima, Department of geosciences, Pennsylvania State University
Shugan Wang, Department of geosciences, Pennsylvania State University

The Marcellus shale is the lowest unit of Devonian age in the Hamilton Group. It is an organic-rich shale located in the Appalachian Basin and contains an estimated ~1.4 trillion cubic meters of natural gas. The majority of gas is held in matrix pore space, with vertical fractures providing additional storage and acting as primary flow pathways. However, commercial production of the gas requires the use of directional drilling and hydraulic fracturing to generate additional permeable pathways. Understanding the response of the Marcellus to stresses created by horizontal drilling and more importantly by hydraulic fracturing is critical for wide-scale commercialization of the resource. We investigated the mechanical behavior of shales from the Marcellus formation, with an emphasis on understanding controls on its rheology and brittle-ductile behavior. We conducted experiments on three lithologies: 1) true "paper shale" (fissile, finely layered) with density $\rho \approx 2.5$ g/cm3 and porosity $\varphi < 5\%$, 2) a low density ($\rho \approx 1.45$ g/cm3) shale with porosity $\varphi = 39.2\%$ (subunit 1), and 3) a lower density ($\rho \approx 1.05$ g/cm3) lithology with porosity $\varphi = 50.8\%$ (subunit 2). We performed experiments on cylindrical samples 25-mm in diameter and 50-mm in length in a triaxial configuration ($\sigma 1 \neq \sigma 2 = \sigma 3$). Samples were deformed using a displacement rate boundary condition (axial strain rates of 2.07e-4 s-1 to 1.63e-2 s-1), and under confining pressures ranging from 0 to 50 MPa. Additionally, we conducted permeability experiments with water (flow through) and helium gas (pulse) at an effective confining pressure of 10 MPa. Our experiments show brittle behavior for the fissile shale unit, including a peak in differential stress, failure, and a stress drop to a residual level. Failure stress shows a systematic increase with confining pressure, typical of brittle behavior. Experiments on subunit 1 show less brittle behavior; the stress-strain curves exhibit a peak stress and post peak strain hardening. With increasing confining pressure, the behavior evolves from brittle to ductile, with an evolution from localized deformation to cataclastic flow. Experiments on subunit 2 show a less brittle behavior, characterized by strain hardening, and we observe compaction with no evidence of localized fracture. Under hydrostatic conditions and with water as the permeant, measured permeabilities of subunit 1 is on the order of 5.5e-15 m2. Pulse-measured permeabilities to non-sorbing gaseous helium are similar to those for water in the order of 8.8e-15 m2.

Sequence Stratigraphic Analysis of the Marcellus Shale and Associated Strata

Daniel R. Kohl
M.S. Student, Petroleum related

Advisor: Dr. Rudy Slingerland

This study presents a sequence stratigraphic framework and depositional model for the Middle Devonian Marcellus Formation and associated strata in Pennsylvania. The dataset consists of eight cores, numerous outcrops, and approximately 1000 wireline well logs throughout central, western, and northern PA. Select outcrops were scanned with a gamma ray scintillometer to produce a spectral gamma ray log comparable to gamma ray well logs. Well logs were normalized using a standard High-Low technique to produce comparable log values among wells, and facilitate accurate correlations of sequence stratigraphic horizons. Sedimentary and sequence stratigraphic observations from proximal facies exposed in outcrop were projected into the subsurface using well log correlation techniques. Cores and outcrop scintillometer profiles were used to map lithofacies to well log facies, enabling prediction of lithofacies from gamma ray logs.

Marcellus shale and associated strata were divided into three depositional sequences and component systems tracts (lowstand (LST), transgressive (TST), and highstand systems tracts (HST)) by observing parasequence and facies stacking patterns. The first depositional sequence is composed of the upper Onondaga Formation and lower Marcellus Formation. Relatively coarse-grained facies of the Onondaga Formation are interpreted to be a LST, and the upper, more fine-grained Onondaga facies are interpreted to represent a TST. Continued deepening led to interfingering of Onondaga limestones with Marcellus black shales as indicated by through-going volcanic ash beds. A maximum flooding surface, picked at the highest gamma ray and lowest density value observed in Marcellus shale marks the start of the HST. In the HST, black shales generally coarsen upwards into calcareous siltstones, and parasequences become less organic rich. Overlying the HST is a generally sharp basinward shift in facies, marking a generally conformable sequence boundary and start of a LST. The upper two depositional sequences of the Marcellus formation are characterized by a relatively coarse grained, low-radioactivity LST. These coarse strata fine upwards into organic-rich, high-radioactivity siltstone representing the TST. Organic rich siltstones generally coarsen upwards in the overlying HST, and the depositional sequence is bounded by a conformable sharp basinward shift in facies.

Maps and cross sections of the sequence stratigraphic framework demonstrate regional facies trends which have implications for petroleum production. Black shales are less radioactive and therefore presumably less organic-rich near depocenters. LST are generally more coarse grained and have higher silt content than TST and early HST deposits. More silt rich strata have superior fracture and borehole stability properties, and are excellent targets for long horizontal well laterals.

Frictional and hydrologic behavior of the San Andreas Fault: Insights from laboratory experiments on SAFOD cuttings and core

Brett M. Carpenter
Ph.D. Student, Post-comps

Advisors: Chris Marone and Demian Saffer

The debate concerning the apparent low strength of tectonic faults, including the San Andreas Fault (SAF), continues to focus on: 1) low intrinsic friction resulting from mineralogy and/or fabric, and 2) decreased effective normal stress due to elevated pore pressure. Here we inform this debate with laboratory measurements of the frictional behavior and permeability of cuttings and core returned from the SAF at a vertical depth of 2.7 km.

We conducted experiments on cuttings and core recovered during SAFOD Phase III drilling. All samples in this study are adjacent to and within the active fault zone penetrated at 10814.5 ft (3296m) measured depth in the SAFOD borehole. We sheared gouge samples composed of drilling cuttings in a double-direct shear configuration subject to true-triaxial loading under constant effective normal stress, confining pressure, and pore pressure. Intact wafers of material were sheared in a single-direct shear configuration under similar conditions of effective stress, confining pressure, and pore pressure. We also report on permeability measurements on intact wafers of fault gouge prior to shearing.

Initial results from experiments show: 1) a weak fault (μ = ~0.1) compared to the surrounding wall rock (μ = ~0.55), 2) velocity strengthening behavior, (a-b > 0), consistent with aseismic slip, 3) near zero healing rates in material from the active fault, and 4) a 2-order of magnitude permeability anisotropy within the fault core. XRD analysis on core indicates the main mineralogical difference between fault rock and wall rock, is the presence of significant amounts of smectitic minerals within the fault rock. Taken together, the measured frictional behavior and clay mineral content suggest that the clay composition exhibits a basic control on fault behavior. Our results document the first direct evidence of weak material from an active fault at seismogenic depths. In addition, our results could explain why the SAF in central California fails aseismically and hosts only small earthquakes.

Abrupt lake level rise of the Siling Co in recent ten years, induced by glacial melting in central Tibet

Xuhua Shi
M.S. Student

Advisor: Eric Kirby

Kai Meng, Institute of Geology and Geophysics, Chinese Academy of Science, China
Eric Kirby, Department of Geosciences, Pennsylvania State University
Erchie Wang, Institute of Geology and Geophysics, Chinese Academy of Science, China
Feng Liu, Institute of Geology and Geophysics, Chinese Academy of Science, China
Kevin Furlong, Department of Geosciences, Pennsylvania State University

Within the Tibetan Plateau are distributed several hundreds of internally-draining brackish lakes of variable sizes. These lakes are least effected by human activities due to their high elevations and remoteness, and therefore are good sensitive recorders of climate change. In this study, we investigate the influence of climate change on lake levels of the Siling Co (Lake) and two smaller neighboring lakes – the Co'e and Bange Co in central Tibetan Plateau. The Siling Co is mainly supplied by glacial meltwater and precipitation primarily supplies the Co'e and Bange Co. Here we analyze 1) variation of lake levels of these lakes during past 34 years and, 2) climate data (precipitation and temperature) collected from meteorological stations around the lakes in the past 50 years. LandSAT remote sensing imagery obtained in same seasons (September - October) are utilized to calculate change of the lake areas of those lakes in past decades. On the other hand, we use digital elevation model (DEM) and differential GPS survey to analyze variation of the lake levels. The results show that 1) an abrupt lake level rise of the Siling Co occurs around 2000. From 1976 to 2000, the lake level is steadily raised by 4.3 m (from 4530 m to 4534.3 m), with an increase rate of 0.18 m/yr. In contrast, from 2000 to 2010, the lake level rise sharply by 8.2 m (from 4534.3 m to 4542.5m), with the rise rate increasing to 0.82 m/yr. Compared with the two-stage lake rise of the Siling Co in the past 34 years, there are only limited rises of lake levels of the Co'e to the southeast and the Bange Co to the east; 2) during this period, the lake area varies consistently with the lake level. The Siling Co shows a rapid increase in lake area during recent 10 years, compared with the steady and slight increase during 1976-1999. By contrast, no significant increase in lake area can be observed from the Co'e and Bange Co.

Analysis of the climate data collected during past decades reveals an increase both in the temperature and precipitation in recent 10 years. However, considering the limited rise of lake levels of the Co'e and Bange Co that are mainly supplied by precipitation and rapid retreating of the source glacials, this study suggests for the first time that the Siling Co rises sharply in recent 10 years and strengthens the previously-proposed idea that increasing glacial melting mainly contributes to lake level rise of the Siling Co.

The effect of Giant Sequoia trees on mineral weathering

Megan Carter
Ph.D. Student, Pre-comps

Advisor: Susan Brantley

Scientists have often studied the complex relationships between climate, erosion, and weathering in an effort to understand long-term landscape evolution, including how landscapes will respond to natural or anthropogenic forcings. Understanding these relationships may prove vital to predicting how climate change could affect particularly vulnerable ecosystems, such as the Giant Sequoia groves of Yosemite National Park. As some of the largest living organisms on earth, Giant Sequoia trees provide a unique opportunity to study the effects of trees on mineral weathering rates, as well as on bulk soil and porewater chemistry. However, as an outlier on the size distribution of tree species, they may be vulnerable to changing patterns of precipitation and temperature.

Furthermore, researchers have identified trees as having an important role in Ca and Mg silicate weathering, which are considered important controls on the long-term global carbon cycle. By producing chelating organic acids and controlling the distribution of soil moisture, plants can alter and even accelerate mineral weathering rates. Furthermore, plant nutrient cycling can result in redistribution of certain elements in the soil profile. To examine these processes, a series of soil cores were collected along a 46 m transect between two mature Sequoia trees in the Mariposa Grove of Yosemite National Park, as well as at a control site well outside the root zone of Sequoia tree specimens. Porewater samples were also obtained from tension lysimeter nests installed along the transect and at the control site weekly to bi-weekly over the course of Summer 2010. Soil samples were analyzed using X-Ray Fluorescence after lithium metaborate fusion. Water samples were analyzed for major cations using Inductively Coupled Plasma-Atomic Emissions Spectroscopy.

Oxides were classified into three categories based on their concentration behavior with depth and compared with porewater chemistry trends with depth. Elemental concentrations in the soil cores were also compared with underlying bedrock composition (El Capitan Granite), in order to identify which elements have been mobilized and redistributed in the soil profile at a range of distances from trees. Na, Ca and P are each fully depleted with respect to parent material from approximately 1 m in depth downward in those soil cores closest to the Sequoia trees. Such a pattern could be consistent with mining of these elements by the tree roots, and uptake and storage in the tree over its approximately 2000 y lifespan. These elements -- especially P -- are less depleted at the surface, an observation that is consistent with recycling of these elements back to the soil profile from tree litter or during fires, etc. A working hypothesis which is consistent with the data is that Sequoias preferentially affect weathering of plagioclase feldspar and apatite within their root zones. Changes in evaporation and precipitation due to future climate change would be expected to be especially important in affecting these patterns.

Solution composition-dependence of the Ca isotope composition of inorganic calcite

Matthew Scott Gonzales
Ph.D. Student, Pre-comps

Advisor: Matthew Fantle

James Watkins, University of California, Berkeley
Donald DePaolo, University of California, Berkeley.

Laboratory experiments have shown that the Ca isotope composition of calcite precipitated from aqueous solution may be sensitive to solution chemistry, temperature, and solution pH. Generally, inorganic calcite precipitation experiments yield calcite crystals that are enriched in the light isotope of Ca relative to the parent solution. Two previous studies by Lemarchand et al. (2004) and Tang et al. (2008) showed that the Ca isotope composition (δ^{44}Ca) of calcite varies systematically with precipitation rate (R). The two studies, however, obtained the opposite relationship between δ^{44}Ca and R despite the fact that both groups precipitated calcite at comparable pH, temperature, and Ca^{2+} as well as CO_3^{2-} ion concentrations. A potentially important difference between the two studies is that Lemarchand et al. (2004) used parent solutions with higher ionic strength (0.85 versus 0.035). The purpose of this study is to determine the solution composition dependence, if any, on Ca isotope incorporation during calcite growth from aqueous solutions.

For our experiments, a beaker containing 300 mL of $CaCl_2$+NH_4Cl solution was placed in container filled with 1 atm of a N_2+CO_2 gas mixture. The degree of supersaturation with respect to calcite was controlled by the pCO_2 of the gas mixture, which was constantly replenished from a gas source. As CO_2 from the atmosphere dissolved into solution, calcite crystals grew on the beaker walls. The pH of the solution was maintained by use of an autotitrator with NaOH as the titrant. Relative growth rates between experiments are determined by weighing the amount of calcite precipitated over the course of an entire experiment on a fixed surface area to provide a first estimate of R.

Experiments thus far have yielded calcite crystals that are enriched in the light isotope of Ca relative to the parent solution by 0.4‰ to 1.6‰. Growth rates are estimated to range from 0.01 to 131 mmol/m^2/hr, overlapping with rates from Lemarchand et al. (2004) and Tang et al. (2008). In experiments where we use a solution with high ionic strength (0.7), we find that δ^{44}Ca in calcite increases with increasing precipitation rate. This is in agreement with the findings of Lemarchand et al. (2004) although Ca isotopes are more fractionated in our experiments. Future work will explore whether a solution with lower ionic strength reproduces the results of Tang et al. (2008), in which δ^{44}Ca in calcite decreased with increasing precipitation rate.

The Role of Grain Caliber in Determining Delta Morphology

Alexander P. Burpee
M.S. Student, Petroleum related

Advisor: Dr. Rudy Slingerland

Delta deposits are important hydrocarbon reservoirs containing an estimated 30% of the world's oil, natural gas, and coal (Tyler and Finley, 1991). Predictions of delta hydrocarbon reservoir connectivity, porosity, permeability, and spatial extent are dependent upon depositional models and increasing the accuracy of these models is important for efficiently exploring for and recovering delta hydrocarbon resources. Current depositional models of ancient deltas are strongly dependent on estimates of a delta's planform morphology. Prior research has identified the role of waves, tides, and river discharge in determining delta morphology, whereas sediment composition and grain caliber have largely been overlooked.

The numerical modeling experiments of Edmonds and Slingerland (2010) first showed the strength of the effect of grain caliber on delta morphology. Using Delft 3D, a complex morphodynamic model, they tested the hypothesis that sediment caliber and discharge have a significant effect on delta morphology. In their experiments, sediment was divided into two sizes: fine-grained and coarse-grained. Fine-grained sediments like clay and silt had cohesive properties and acted to improve channel bank stability and resistance to erosion, while coarse-grained sediments lacked these cohesive properties and channel banks were more prone to erosion. Their numerical experiments demonstrated a systematic relationship between grain size and morphology where deltas dominated by fine-grained sediment resulted in "bird's foot" shapes and deltas dominated by coarse-grained sediment resulted in "fan" shapes.

This thesis seeks to test the Edmonds and Slingerland (2010) result by surveying the grain sizes and morphologies of modern and ancient deltas. Specifically, I will test the following hypothesis:
> If a delta topset deposit consists of a high silt and clay to sand ratio, then the delta will have an environmentally more complex delta plain that will produce greater shoreline rugosity, lower bifurcation angles, lower clinoform dip magnitudes, and less sand-body connectivity than deltas with sandier topsets.

If the hypothesis can not be rejected, I will reclassify deltas based on their grain caliber as well as external forcing by waves, tides, and river discharge.

^{40}Ar/^{39}Ar Dating of Basalt Flows Capping the Tertiary Brown's Park Formation Provide New Constraints on the Neogene Incision and Uplift History of the Yampa and Little Snake Rivers, Colorado

Russell Rosenberg
M.S. Student

Advisor: Eric Kirby

The topography of the Western Rocky Mountain Region of Colorado is characterized by a network of deeply incised channels and regions of high topography. Deeply incised topography is especially apparent along the Colorado River in several locations as it drains the Western Rockies. Previously collected incision datums for the Colorado River suggest that the Colorado River has incised approximately 1.5 km into bedrock over the last 10 Ma at Glenwood Canyon. Several possible drivers for this incision have been suggested; including Pliocene climate changes and transient incision associated with drainage integration downstream. We suggest that regions of high topography in the Colorado Rockies are being supported by areas of mantle buoyancy suggested by previously imaged zones of slow P-wave velocities. Geophysical data suggest that mantle influence on topography should be more prevalent along the Colorado River as compared to the Yampa, Little Snake, and Green Rivers further to the north. ^{40}Ar/39Ar dates on basalts capping the Tertiary Browns Park formation, which we interpret to represent a deposition surface until c.a. 8-10 Ma, provide new incision datums along the Little Snake and Yampa Rivers which yield incision magnitudes of approximately 0.5 km over the last 8-10 Ma. Additionally, preliminary analysis of normalized channel steepness within the Colorado and Yampa River watersheds agree to a first order with spatial patterns of incision. These observations suggest that high, deeply incised, topography in the Western Rockies is dominantly supported by the underlying mantle structure.

An experimental investigation of multiple sulfur isotope fractionations during heterogeneous reactions between SO_2 and activated carbon

Hiroshi Hamasaki
M.S. Student

Advisor: Dr. Hiroshi Ohmoto

Dr. Yumiko Watanabe, Penn State Astrobiology Research Center

We have conducted four series of experiments to investigate S isotope effects during different stages of reactions (e.g., adsorption, redox reactions) between activated carbon and SO_2 gas. The experiments were conducted in a specially constructed Pyrex-glass system where known amounts of SO_2 gas and activated carbon were heated together at 200°C (or 250°C), and aliquots of SO_2 gas were periodically withdrawn for isotopic analyses. At the end of experiments, the solid reaction products were investigated for chemical and isotopic compositions.

Following are the important findings from our investigation:
(1) Isotopic equilibrium was readily established between the adsorbed SO_2 on the activated carbon and free SO_2 gas within 1 hour; the isotopic fractionation factor α ($SO_2(ads) - SO_2(g)$) is 1.00332 at 200°C and 1.00485 at 250°C,

(2) The $\Delta^{33}S$ (= $\delta^{33}S_i - 0.515x\ \delta^{34}S_i$) values of the adsorbed SO_2 and gaseous SO_2 are all within 0±0.08 ‰, indicating that the isotopic fractionation during the chemisorption reactions in our experiments was mass dependent ($\Delta^{33}S <\pm0.2$). This agrees with a theoretical prediction by Lasaga et al. (2008) that anomalous (or mass-independent) fractionation of sulfur isotopes occur only when the chemisorption energy is less than ~30 kJ/mol; the chemisorption energy between activated carbon and SO_2 gas is usually in a range of 13 to 80 kJ/mol.

(3) Several sulfur species formed during the series of adsorption experiments. Sequential sulfur extraction out of the solid reaction products by HCl, Cr-reductive solution, and KIBA solution revealed the presence of significant amounts of water soluble S (e.g., sulfates), Cr-reducible S compounds (e.g., polysulfides) and non Cr-reducible S compounds (e.g., C-S compounds), indicating that some of the adsorbed SO_2 underwent redox reactions by the carbon. Multiple S isotope values of those sulfur species product were mass dependently fractionated.

Lasaga et al. Anomalous fractionation of sulfur isotopes during heterogeneous reactions. Earth And Planetary Science Letters (2008) vol. 268 (1-2) pp. 225-238

Laboratory Observations of Ice's Deformational Properties

Lucas Zoet
Ph.D. Student, Pre-comps

Advisor: Sridhar Anandakrishnan

Richard B. Alley, Pennsylvania State University
Chris Marone, Pennsylvania State University

In recent studies large ($M_w > 1$) seismicity has been found to originate from the base of glaciers near the Ice bed region. The exact interface generating the seismicity is difficult to isolate with current seismic techniques, however the most logical location, which could generate events of this magnitude, is the area where debris-laden ice slides over a consolidated bed. This interface is difficult to reach in the field as well as demanding to access for measurements. The Rock Mechanics Laboratory at Penn State University provides a unique apparatus, which allows exertion of a normal stress equivalent to ice at the base of a glacier, as well as application of a driving stress near observed values. The precise control of the apparatus allows us to isolate pertinent variables in order to better constrain their relevance to the subglacial environment.

In order to study how changes in entrained debris affects deformation of ice; we froze a number of ice samples with varying amounts of debris between 1-60% by weight. These samples of ice were sheared in a single direct shear apparatus against a piece of Westerly granite at velocities ranging from 3 to 300 microns per second under a normal load of 1.25 MPa. Frictional values were recorded for each sample of ice. Slide-hold-slide experiments were conducted, which report that an increase in hold time increased the strength of the ice, indicating healing was taking place. Velocity stepping tests were conducted showing a transition from a velocity strengthening to a velocity weakening material near a velocity of 10 microns per second. The transition had secondary effects imposed from the amount of debris contained within. We suggest that this measurement is compatible with our observations of the slipping behavior of David Glacier. Next, the stiffness of the shearing apparatus was reduced using springs to allow stick-slip behavior to occur at the low normal stresses (500 kPa) and shear stresses (150 kPa) that were used in the experiment. We successfully produced stick-slip behavior in the lab. Similarities between laboratory results and field observations are beginning to emerge which will help to scale from the one to the other.

The crustal structure of East Africa

Fred Tugume
Ph.D. Student, Post-comps

Advisor: Andrew Nyblade

Jordi Julia

Broadband data from 40 seismic stations deployed in Uganda and western and southern Tanzania between 2007 and 2010 have been used to investigate crustal structure in parts of East Africa, where little is known about the nature of the crust. P wave receiver functions generated using data from several hundred teleseismic earthquakes have been combined with Rayleigh wave group velocity measurements to invert for the S wave structure of the crust and uppermost mantle beneath each seismic station. Moho depths of about 35-40 km are obtained for almost every station outside of the rift valleys, with little difference in crustal structure apparent between the Archean Tanzania Craton and Proterozoic mobile belts to the west of the craton. The crust appears to be somewhat thinner beneath the rift valleys in the western branch of the East African rift system. However, results from rift stations are not as reliable because reverberations from the bottom of the sedimentary basins make the receiver functions difficult to model. The new results are combined with results from previous studies of crustal structure in East Africa to produce a map of crustal structure across most of East Africa.

Understanding arc magma evolution in thick continental crust

Timothy T Murray II
Ph.D. Student, Pre-comps

Advisor: Maureen Feineman

Located in northern Southern Volcanic Zone (SVZ) of the Andes, the Diamante Caldera - Maipo volcanic complex (DMC) consists of the Diamante caldera, 16x20 km in diameter, and Maipo Volcano, an andesite/dacite stratovolcano straddling the border between Chile and Argentina. The northern part of the SZV is characterized by exceptionally thick continental crust (>50 km) (Sruoga et al. 2005), thus we might anticipate that the magmas in this region would experience extensive crustal interaction prior to eruption. Whole rock major element data was obtained using standard lithium metaborate fusion sample preparation techniques and then analyzing the samples by inductively coupled plasma atomic emission spectroscopy (ICP-AES). Cyclical variability in silica content, 54% to 68%, suggests magma mixing as a result of magma recharge in an upper crustal magma chamber. Modal analysis shows that the dominant lava type erupted at Maipo is plagioclase-phyric andesite and dacite, with subordinate hornblende-phyric dacite found only at a single ring fracture dome. Trace element and isotopic evidence suggests at least two magma-stalling episodes within the underlying continental crust. Evidence for garnet fractionation (Sr/Y ratios up to 37) in basaltic andesites suggests fractional crystallization and stalling in the lower crust, as garnet is only stable at depths >~35 km (Drew et al 2011). More evolved lavas show petrological and geochemical evidence of assimilation and fractional crystallization in the upper crust, such as ingrowth of a strong negative Eu anomaly as the result of plagioclase crystallization in a shallow magma chamber. Due to this extensive crustal interaction, ongoing geochemical and petrological analysis will help further illuminate time-scales for magma recharge in this area, crustal contamination during stalling events, and will allow us to compare magma evolution at contrasting pressures and temperatures in the crust. Future work will include mapping and sampling on the western (Chilean) flank of Maipo, as all of the recent field work has been conducted on the Argentine side.

Sruoga, P., et al. 2005. Volcanological and geochemical evolution of the Diamante Caldera–Maipo volcano complex in the southern Andes of Argentina (348100S). Journal of South American Earth Sciences 19 p. 399-414

Drew, D., et al. Unpublished data. State College, Pa.: The Pennsylvania State University.

Oral Session One:
Mineralogy and Geochemistry

Saturday, March 19
8:45-10:00 am, 114 EES

Time	Presenter	Advisor	Title
8:45	Kristina Peterson	Peter Heaney	Time-resolved X-ray diffraction study of the in situ hydrothermal phase transformation from akaganéite to hematite
9:00	Claire Fleeger	Peter Heaney	Determining the rate of Cs sequestration by hexagonal H-birnessite and triclinic Na-birnessite as a function of pH
9:15	Elizabeth Herndon	Susan Brantley	Understanding manganese biogeochemistry on a watershed-scale using molecular spectroscopy
9:30	Tiffany Yesavage	Susan Brantley	Fe cycling in the Shale Hills Critical Zone Observatory, Pennsylvania: An analysis of microbiology, chemical
9:45	Ashlee Dere	Susan Brantley and Tim White	Shale weathering across a continental-scale climate gradient

Time-resolved X-ray diffraction study of the *in situ* hydrothermal phase transformation from akaganéite to hematite

Kristina Peterson
Ph.D. Student, Post-comps

Advisor: Peter J. Heaney

Jeffrey E. Post, Department of Mineral Sciences, Smithsonian Institution

Akaganéite nanoparticles commonly form when chlorine-rich fluids alter metallic Fe, and recently they have been discovered as a biogenic product. Although the precipitation of akaganéite (β-FeOOH, Cl) and its subsequent transformation to the stable phase hematite (α-Fe_2O_3) are well documented, the mechanism and the kinetics of this reaction are debated. The difficulty in characterizing the transformation can be attributed in part to the poorly crystalline nature of most natural akaganéite. Additionally, *in situ* analysis is challenged by the low precipitate yield in hydrothermal experiments within the Fe-Cl-H_2O system.

Here we present new observations from *in situ* heating experiments using time-resolved synchrotron X-ray diffraction (TR-XRD) conducted at the Advanced Photon Source (APS). Starting with ferric chloride solutions (0.45 M $FeCl_3$ + 0.01 M HCl), we have collected TR-XRD data of the hydrothermal precipitation of akaganéite and transformation to hematite. Design of a new heater and experimental protocol facilitated our collection of *in situ* data by precipitate sedimentation at the base of a sealed 0.7 mm quartz capillary. XRD data were collected every 30 seconds at temperatures ranging from 80-200°C. Rietveld refinements using the General Structure Analysis System (GSAS) allowed for quantitative measurements of reaction rates as a function of temperature. Moreover, we determined the dependence of unit cell parameters on temperature and particle size.

In our experiments, the akaganéite to hematite transformation was completed in 100, 20 and 4 minutes at temperatures of 150°C, 175°C and 200°C, respectively. Refined unit-cell parameters for each phase followed the same general trends at all temperatures. Lattice parameters of akaganéite did not significantly change throughout the reaction. The hematite *a* parameter decreased with increasing particle size, but the *c* parameter increased until all akaganéite had transformed, after which it decreased. Our results demonstrate that *in situ* structural and kinetic data of low-yield hydrothermal reactions can be successfully captured using our experimental design and TR-XRD.

Determining the rate of Cs sequestration by hexagonal H-birnessite and triclinic Na-birnessite as a function of pH

Claire R. Fleeger
Ph.D. Student, Post-comps

Advisor: Peter J. Heaney

Jeffrey E. Post, Department of Mineral Sciences, Smithsonian Institution

High-level nuclear waste storage tanks at the DOE Hanford site in Richland, Washington have leaked more than 1 million gallons of solution that is extremely basic (pH > 13) with high ionic strength and concentrated in radioactive Cs-137 (2×10^{10} Bq/L, equivalent to 0.04 mmol/L). The underlying Ringold Formation consists of poorly consolidated clays, silts, and sands rich in Fe and Mn oxides, including the phyllomanganate birnessite. Time-resolved synchrotron X-ray diffraction (TR-XRD) and inductively coupled plasma-mass spectrometry (ICP-MS) were used to measure the kinetics and mechanisms of Cs substitution for interlayer Na^+ and H^+ in birnessite at pH values ranging from 3 to 10. These data demonstrate that Cs exchange rates decrease as pH increases, but the amount of Cs that will exchange into the interlayer is dramatically higher as pH increases. This behavior was observed in both hexagonal and triclinic birnessite.

Understanding manganese biogeochemistry on a watershed-scale using molecular spectroscopy

Elizabeth Herndon
Ph.D. Student, Post-comps

Advisor: Susan Brantley

Manganese contamination in soils is prevalent in industrialized regions (Herndon et al., 2011). Over the past few centuries, large quantities of Mn have been extracted from the lithosphere, emitted to the air via anthropogenic activities, and redeposited to the Earth's surface. In order to evaluate environmental impacts of Mn deposition, we must better understand the biogeochemical behavior of Mn in soils. Vegetation can act as an element capacitor, storing large quantities of Mn and releasing it slowly into the environment over time. The mechanisms of Mn uptake into vegetation and eventual release to soils through decomposition are unclear. Here, we use spectroscopic techniques to characterize Mn-compounds in major reservoirs of a contaminated watershed. We find that Mn-oxidation during leaf decomposition may immobilize and retain Mn within contaminated soils.

Characterization of Mn-compounds in the environment is often limited by their high reactivity and poor crystallinity. Synchrotron source radiation can be used to map the microscale distribution of Mn (**X**-**R**ay **F**luorescence) and identify its local chemical environment (**X**-ray **A**bsorption **F**ine **S**tructure spectroscopy) in natural samples. We use XRF and XAFS to characterize the spatial abundance and chemical forms of Mn in mineral soil, organic soil, and tree leaf samples from both the field and a controlled greenhouse experiment.

XAFS results indicate that Mn is reduced (Mn^{+2}) and organically-complexed in bulk leaf tissue, but present as a mixed-valence oxide ($Mn^{+3/+4}$) similar to birnessite and todorokite in organic and mineral soils. This result is consistent with uptake of reduced Mn from soil by trees and subsequent Mn-oxidation as tree leaves fall and decompose in the soil. Furthermore, XRF analysis of leaves from trees exposed to high Mn reveals that the Mn is concentrated in visible dark spots. These dark concretions contain organically-complexed, trivalent Mn. Mn^{+3} is thought to be unstable in the environment and is used as a reactive catalyst in lignin degradation. Therefore, the presence of abundant Mn^{+3} in fresh leaves may enhance rates of litter decomposition (Berg et al., 2007). More detailed studies are needed to elucidate the mechanisms underlying these Mn redox reactions; however, we find that Mn undergoes chemical transformations during biotic cycling that may increase its residence time in soils and impact decomposition reactions.

Herndon, E.M., Jin, L., Brantley, S.L. (2011) Soils reveal widespread manganese enrichment from industrial inputs. *Environ. Sci. Tech.* **45**(1): 241-247.

Berg, B., Steffen, K.T., McClaugherty, C. (2007) Litter decomposition rate is dependent on litter Mn concentrations. *Biogeochem.* **82:** 29-39.

Fe cycling in the Shale Hills Critical Zone Observatory, Pennsylvania: An analysis of microbiology, chemical weathering, and Fe isotope fractionation

Tiffany Yesavage
Ph.D. Student, Post-comps

Advisor: Susan L. Brantley

Laura J. Liermann, Department of Geosciences, The Pennsylvania State University
Matthew S. Fantle, Department of Geosciences, The Pennsylvania State University
Lixin Jin, Department of Geosciences, The Pennsylvania State University
Jeffrey Vervoort, School of Earth and Environmental Sciences, Washington State
       University
Ryan Mathur, Department of Geology, Juniata College

During the process of chemical weathering, iron (Fe) shows complex behavior driven by both abiotic and biotic processes. The goal of this study is to understand Fe transformations in the Shale Hills watershed of Central Pennsylvania, which is developed almost entirely on an organic-poor marine shale. Regolith samples were collected from a planar hillslope on the south side of the catchment where the flow of water is assumed to be non-convergent. Concentrations of Fe plotted versus depth along the transect indicate that total iron and Fe(II) are depleted in regolith samples relative to an immobile element in the bedrock, consistent with moderate, incomplete losses of both total Fe and Fe(II) during weathering. Exceedingly low Fe concentrations in lysimeter samples are consistent with Fe loss as fine particulates. Furthermore, Fe-reducing bacteria are only abundant in the wetter valley floor, while the distribution of Fe-oxidizing bacteria was highest both in surface horizons and along the soil/bedrock interface. Although the extent of Fe isotopic fractionation is small, both bulk Fe and HCl-extracted Fe in regolith become increasingly depleted in ^{56}Fe relative to bedrock with increased weathering. As this finding is inconsistent with predictions based on published laboratory experiments incorporating ligand-promoted dissolution or dissimilatory Fe-reducing bacteria, we infer that these mechanisms are of limited importance in fractionating Fe isotopes at this site. Instead, this study is consistent with loss of isotopically heavy colloidal Fe from the watershed, resulting in residual regolith that becomes increasingly light as weathering proceeds.

Shale weathering across a continental-scale climate gradient

Ashlee Dere
Ph.D. Student, Pre-comps

Advisor: Sue Brantley and Tim White

Both ecosystems and humans are dependent on soil for nutrient and water cycling as well as food, making the loss of soil a major issue facing humanity. However, the rate at which soil forms (replacing what is lost) is not well understood. To investigate rates of soil formation in various climates, a latitudinal climosequence of forested sites has been established in North America and Wales. All sites are underlain by an organic-poor, iron-rich (Silurian-age) shale, providing a constant parent material from which soil is forming. The climosequence is bounded by a cold/wet end member in Wales and a warm/wet end member in Puerto Rico; in between, temperature and rainfall increase as sites extend south through New York, Pennsylvania, Virginia, Tennessee and Alabama. Soil sampling and geochemical analyses, which provide a snapshot of shale weathering with depth, were completed similarly at all sites to allow direct comparisons and eventual modeling of the shale weathering processes. In addition, instrumentation deployed at each site gathers basic meteorology and soil moisture and temperature measurements providing present-day climate data for each soil. Initial results show soil depth increases as a function of temperature but is not correlated with precipitation. Chemical depletion profiles of Mg, which approximate chlorite and illite dissolution, show deeper weathering fronts at warmer sites. Similarly, Na, a proxy for feldspar dissolution, shows greater depletion in warmer climates. Overall, data collected from soils across the transect will promote a better understanding of how climate changes and human activities impact soil formation rates.

Oral Session Two A:
Biogeochemistry

Saturday, March 19
10:15 am-12:15 pm, 114 EES

Time	Presenter	Advisor	Title
10:15	Brendan Puls	James Kubicki	Structural and Functional Analysis of Flavins Secreted by S. Oneidensis during Microbial Iron Reduction
10:30	Heath Watts	James Kubicki	Untangling Lignin with Quantum Mechanics
10:45	Rebecca McCauley	Jennifer Macalady	Metabolic Strategies in Energy-Limited Microbial Communities in the Anoxic Subsurface (Frasassi Cave System, Italy)
11:00	Katherine Dawson	Jenn Macalady and Kate Freeman	Molecular characterization of archaeal lipids across a hypersaline gradient
11:15	Heather Graham	Kate Freeman	Foliar Stable Isotope Dynamics In a Closed-Canopy Tropical Forest: Towards a Better Understanding of Terrestrial Productivity in the Past
11:30	Laurence Bird	Kate Freeman	F430, Understanding Methanogenesis and methane rich environments
11:45	Clayton Magill	Kate Freeman	Monsoon intensity and ecosystem change in eastern Africa during the emergence of the genus Homo
12:00	Elizabeth Denis	Kate Freeman	A Fiery Investigation of the Paleocene-Eocene Thermal Maximum (PETM)

Structural and Functional Analysis of Flavins Secreted by *S. Oneidensis* during Microbial Iron Reduction

Brendan Puls
Ph.D. Student, Pre-comps

Advisor: James Kubicki

Ming Tien, Pennsylvania State University
Josh Stapleton, Pennsylvania State University

Flavin mononucleotide (FMN) and riboflavin are each secreted by *S. oneidensis* during extracellular electron transfer and increase the rate of electron transfer by interacting with reducible iron and/or shuttling electrons between outer-membrane cytochromes and iron-oxide minerals (Canstein et al., 2008; Marsili et al., 2008). In our study, we use quantum chemical calculations and infrared spectroscopy to analyze the structures and functions of these flavins. Our goals are to 1) resolve the binding structures of FMN and riboflavin with aqueous Fe^{3+} and iron-oxide nanoparticles, 2) predict the functional difference between the isoalloxizine groups and different tail groups of FMN and riboflavin, and 3) predict the functional difference of FMN and riboflavin in extracellular electron transfer. We use infrared spectroscopy to measure the vibrational spectra and quantum chemistry to calculate the minimum energies and expected infrared peaks for several structural configurations of each flavin. We then compare the measured spectra and the calculated minimum energies and peaks to analyze the binding structure and extracellular function of each flavin. Our results so far indicate that flavin-iron binding is only favored at the tail phosphate group of FMN, leaving aqueous riboflavin to shuttle electrons between the bacterium and the iron-oxide. Further measurements and more precise calculations are in progress to better determine the nature of this binding. This study is the first step towards describing the extracellular role of flavins on a molecular level.

Canstein H. et al. (2008) Secretion of flavins by *Shewanella* species and their role in extracellular electron transfer. *Appl. Environ. Microbiol.* 74, 615-623.

Marsili E. et al. (2008) *Shewanella* secretes flavins that mediate extracellular electron transfer. *PNAS* 105, 3968-3973.

Untangling Lignin with Quantum Mechanics

Heath D. Watts
Ph.D. Student, Post-comps

Advisor: James D. Kubicki

Coniferyl alcohol (MG) is a monomeric constituent of the lignin, the second most abundant biopolymer. Lignin is recalcitrant to removal from plant cell walls and is responsible for rigidity and water conduction in terrestrial plants; thus, lignification was a crucial step in terrestrial plant evolution. The polymer is also a major constituent of lignite (brown) coal.

Consequently, better understanding of lignin structure could aid plant degradation methods for biofuel production,[1] and will provide additional knowledge about plant and coal chemistry. Quantum chemical calculations are useful for confirming, verifying, and predicting data from complicated chemical structures. For this work, ^{13}C NMR calculations were performed on MG and four of its dimers to compare the calculated chemical shifts with experimental data.[2] If observed dimer linkages can be calculated accurately, then the technique could be applied to larger lignin polymers.

Energy-minimization of six conformers of MG were followed by thermodynamically-averaged NMR calculations; these calculations provided excellent statistical agreement with experimental ^{13}C NMR data.[3] Further, thermodynamically-averaged, multi-standard NMR calculations for four MG dimers provided superb statistical agreement with experiment (Figure 1). These results may be useful for elucidating complex lignin NMR spectra and for lignin stability studies.

References

1. Liang, H.; Frost, C.; Wei, X.; Brown, N.R.; Carlson, J.E.; and Tien, M. *Clean-Soil, Air, Water.* 2008, 36(8), 662-668.
2. Lignin NMR database: http://ars.usda.gov/Services/docs.htm?docid=10491
3. Sarotti, A.M; Pellegrinet, S.C. *Journal of Organic Chemistry.* 2009, 74, 7254-7260.

Figure 1: Results for the 5-5 MG dimer *vs*. experiment. Error bars show RMS error.
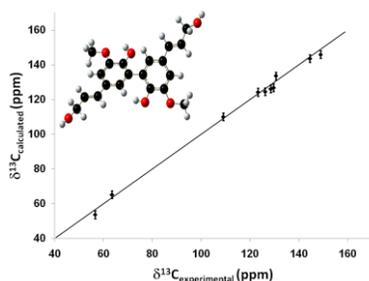
Metabolic Strategies in Energy-Limited Microbial Communities in the Anoxic Subsurface (Frasassi Cave System, Italy)

Rebecca McCauley
Ph.D. Student, Pre-comps

Advisor: Dr. Jennifer Macalady

D. S. Jones, Penn State
I. Schaperdoth, Penn State
L. Steinberg, Penn State

An unusual biofilm with rope-like morphology was recovered by divers from the anoxic and sulfidic water of a remote cave lake (Lago Infinito). The biofilm has high species richness, and is dominated by *Deltaproteobacteria* and *Chloroflexi*. *Deltaproteobacteria* in sulfate-reducing clades make up a significant fraction of the community, consistent with geochemical data and thermodynamic calculations showing that sulfate reduction is highly favorable. *Chloroflexi* in organoheterotrophic clades are also significant populations. BLASTx of metagenomic reads to the NCBI non-redundant database confirm the importance of *Chloroflexi* and *Deltaproteobacteria*, and highlight considerable database bias. In addition to dissolved organic carbon (5 µM as acetate; >1ppm C) and sulfide (175 µM), ammonium (100 µM), and H_2 are plausible electron donors. However, electron acceptors other than sulfate (1.6 mM) are non-detectable (NO^{3-}, NO2-, Fe3+, Mn4+). Roughly 1/3 of the 16S rRNA fragments retrieved from the biofilm have no cultivated relatives at the order or phylum level. Data collected to date indicate that this system is likely to reveal new links between sulfate cycling and microbial lineages with no cultivated representatives.

Molecular characterization of archaeal lipids across a hypersaline gradient

Katherine S. Dawson
Ph.D. Student, Post-comps

Advisors: Jenn Macalady and Kate Freeman

Mathew Rhodes, Department of Geosciences, Penn State
Christopher House, Department of Geosciences, Penn State

Through changes in water usage and weather patterns, the surface level of the Dead Sea decreased by 30 meters, over the past 60 years. A water channel diverting water from the Red Sea, with a salinity of 40 g l^{-1}, to the Dead Sea, with a current salinity of 340 g l^{-1}, is a proposed solution. A series of experimental pools have been set up to study the potential ecological consequences of this alteration in water chemistry. Here we examine the archaeal lipid composition of four pools with varying mixtures of Dead Sea and Red Sea water, as well as halophilic archaeal isolates grown at varying NaCl concentrations. APCI-HPLC-MS analysis shows the prevalence of diphytanyl glycerol diether lipids (DGD's), characteristic of a halophilic archaeal dominated community and a geologically relevant biomarker. Molecular analysis of DGD structure by GC-MS spectroscopy indicates the presence of several core lipids structures consistent with the unsaturated phytanyl and sesterpanyl chains. In the environmental samples, the relative abundance of unsaturated structures shows an inverse relationship to the salinity, while laboratory grown isolates show a positive relationship. We hypothesize that the observed changes in environmental samples are due a shift in the microbial community rather than a physiological response to ambient salinity.

Foliar Stable Isotope Dynamics In a Closed-Canopy Tropical Forest: Towards a Better Understanding of Terrestrial Productivity in the Past

Heather V. Graham
Ph.D. Student, Pre-comps

Advisor: Kate Freeman

Scott L. Wing, Smithsonian Institution

Tropical forests with closed canopies today represent a large proportion (~40%) of global terrestrial biomass carbon, at least one-third of global soil carbon and 30-50% of terrestrial productivity. However, productivity of terrestrial habitats in the past is difficult to discern from the fossil record and the geologic history of three-dimensional forest structure remains unknown. This study seeks to identify isotopic and biochemical leaf characteristics that signify a closed canopy forest and are preserved in the geologic record. The most charismatic feature of dense canopy forests is the extreme light gradient from canopy top to base, with as little as 1% of available light reaching the forest floor. Along this gradient, leaves exhibit strong light-dependent physiological responses and these adaptations are recorded in biochemical and anatomical leaf features. Using the canopy crane access system at Bosque Protector San Lorenzo in Panamá we have sampled leaves in the full diversity of light environments available in a lowland, *terre firme* rainforest.

As expected, bulk leaf material and plant waxes reveal a well-known pattern of vertical enrichment of carbon isotopes. This is generally attributed either to ^{13}C-depleted carbon dioxide from respiration in the understory or to the increased photosynthetic rate typical of high light leaves. By comparing bulk leaf ^{13}C to air samples captured in the same sampling locations we are able to contrast the effects of light with air ^{13}C composition. Vertical gradients in the deuterium composition of leaf-water are associated with the evapotranspirative pattern of enrichment in high light leaves. We measured the D/H ratios of extracted *n*-alkanes to see if this relationship extends to geologically recalcitrant leaf wax lipids. Likewise, $\delta^{18}O$ of cellulose was determined to test if evaporation in the canopy forest and confirm the effects of humidity on the oxygen isotopic composition of cellulose. Lipid composition and abundance also correlates with light environment with shade leaves producing, on average, longer alkane chains. A better understanding of light-sensitive features and their biases in preserved biomarkers is essential to identifying closed-canopy, low-light forest environments and interpreting forest architecture and terrestrial productivity in the fossil record.

F430, Understanding Methanogenesis and methane rich environments

Laurence Bird
Ph.D. Student, Pre-comps

Advisor: Kate Freeman

Jamey Fulton, Pennsylvania State University

Large amounts of methane are oxidized to carbon dioxide by communities of methanotrophic archaea and sulphate reducing bacteria, preventing this greenhouse gas from reaching the atmosphere. Recently evidence has emerged that methyl-coenzyme M reductase can catalyze the anaerobic oxidation of methane. F430, a nickel coenzyme complex is contained within the active site of methyl-coenzyme M of methanogens and appears to be used in both methanogenesis and methanotrophy. Evidence has mainly come from pure culture analysis. Here we provide evidence for F430 in both environmental samples from methane seeps in the Gulf of Mexico and coastal California, enrichment cultures from Bear Meadows Bog as well as pure cultures of *Methanosarcina acetivorans.* Using a modified method F430 has been extracted and identified using LC-MS with nano-EA providing isotopic data for carbon and nitrogen. The identification of F430 in environmental samples is particularly important as it provides evidence for anaerobic methane oxidation in a low oxygen environment via the reversal of the enzymes involved in methanogenesis. This data warrants further exploration for F430 in other anoxic methane seep environments both past and present. Sampling could be conducting at sea floor methane seep and at ancient methane seeps due to the stability of similar porphyrin structures, though the preservation of distinctive, F430-derived porphyrins is currently unknown. A variety of complimentary techniques could also be implemented into the study of F430, particularly intramolecular isotope analysis and metagenomics. Both may go someway to reveal more information on the use of this coenzyme in methanogenic archaea and their relationship to sulfate reducing bacteria. Identification of F430 in anaerobic environments has implications beyond the field of geomicrobiology by providing insight into the methane cycle on the Earth and a way microbes elsewhere in the solar system may produce and consume methane.

Monsoon intensity and ecosystem change in eastern Africa during the emergence of the genus *Homo*

Clayton R. Magill
Ph.D. Student, Post-comps

Advisor: Dr. Katherine Freeman

Environmental hypotheses of human evolution directly link adaptive junctions with patterns of aridification, but the timing and mechanism(s) governing the influence of climate change on our ancient ancestors remains elusive. Here we present new records of hydroclimate and ecosystem change at Olduvai Gorge – the "Cradle of Mankind" – during an epoch associated with the appearance and dispersal of the genus *Homo*, ~2.0 million years ago (Ma) to 1.8 Ma.

We measured the carbon isotope composition of bulk organic matter ($\delta^{13}C_{TOC}$) and leaf-wax biomarkers ($\delta^{13}C_{wax}$), and molecular deuterium ratios (δD) for ancient lake and soil sediments. Values of $\delta^{13}C_{TOC}$ range ~10‰ and couple strongly with Earth's angle of axial precession. Similarly, $\delta^{13}C_{wax}$ correlates strongly with precession, but fluctuates between ~-22‰ and -36‰. We estimated the relative abundance of plant functional groups (*i.e.*, C_3 and C_4) using isotopic trends observed in modern African ecosystems, in order to account for variable biosynthetic fractionation of deuterium by plants. Interpolated δD values of environmental waters, based on measured δD values of leaf-wax biomarkers, are enriched (5‰) and depleted (-40‰) during times of maximum C_4 and C_3 abundance respectively.

We interpret these results as evidence of pronounced environmental variability in eastern Africa during the early Pleistocene that was guided by patterns of tropical insolation. Our rainfall reconstructions indicate ~350 mm decreases in precipitation that occurred on millennial timescales. When considered in the context of the hominid fossil record, our data indicate evolutionary events may have been mediated by environmental variability.

A Fiery Investigation of the Paleocene-Eocene Thermal Maximum (PETM)

Elizabeth Denis
Ph.D. student, Pre-comps

Advisor: Kate Freeman

Past hyperthermal events, such as the Paleocene-Eocene Thermal Maximum (PETM), can serve as analogs for current and future climate changes. About 55.8 Ma during the PETM, a significant amount of CO_2 was released in less than 10 ky and global temperatures increased by 5-9°C over a span of $100 - 200$ ky. This event coincided with a global negative carbon isotope excursion, suggesting a massive perturbation to the global carbon cycle and a large release of ^{13}C-depleted carbon to the atmosphere, oceans and biosphere. Several proposed sources of this carbon include ocean-floor clathrates, thermogenic methane, and burning of peat and/or shallowly buried coal, but the exact source(s) remain unknown. The Paleocene was a time of extensive terrestrial organic carbon burial and some authors have suggested that a change in climate induced burning of the ^{13}C-depleted carbon deposits. Understanding the source and amount of carbon released during the PETM provides constraints on climate sensitivity to CO_2, which is critical for evaluating the response of the Earth system to current anthropogenic changes to the carbon cycle.

Previous work has established that low molecular weight (LMW) PAHs can serve as indicators of local fire events (within 0.5 km) and can be used to detect fires in the paleorecord. In this study, PAHs and charcoal will be used to investigate the occurrence of fire during the PETM from outcrop and long core samples from the Bighorn Basin, WY. The Bighorn Basin preserves one of the most complete terrestrial records of hyperthermal events in the world and encapsulates upper Paleocene to lower Eocene rocks for both pre- and post- PETM analyses. PAH abundance will be measured using high performance liquid chromatography. By comparing the relative abundance of PAHs from the late Paleocene through the early Eocene, temporal variations in fire occurrence will be evaluated. I hypothesize that climate-induced burning will be evident in these Paleocene-Eocene sediments as indicated by an increase in LMW PAHs during the PETM. This study will provide a fire record for the late Paleocene and early Eocene and help constrain climate sensitivity during a warm, CO_2-rich climate.

Oral Session Two B:
Petrology and Geodynamics

Saturday, March 19
10:15 am-12:15 pm, 116 EES

Time	Presenter	Advisor	Title
10:15	Alicia Cruz-Uribe	Maureen Feineman	From Microns to Mountains: Using diffusion models to measure reaction rates in metamorphic rocks
10:30	Megan Pickard	Tanya Furman	Geochemical Insights into Multi-component Mantle Beneath the Anatolian Plate
11:45	Halldor Geirsson	Peter LaFemina	Constraints on the magma plumbing system of Hekla volcano, Iceland, from geodetic GPS measurements
11:00	Rachel Piotrschke	Kevin Furlong	Insights into the Tectonic Development of the Klamath Mountains Province from Thermal Data and Modeling
11:15	Brett Carpenter	Chris Marone and Demian Saffer	Insights into the frictional and hydrologic behavior of the Alpine Fault, West Coast, South Island, New Zealand
11:30	Bryan Kaproth	Chris Marone	Quantifying pressure solution and lithification: tying elastic moduli measurements to changes in porosity and deformation style in sheared granular aggregates
11:45	Christine Regalla	Donald Fisher and Eric Kirby	Exhumational and incisional response to active faulting in the Japanese forearc, northeast Honshu
12:00	Nicole West	Eric Kirby	Using meteoric ^{10}Be as a tracer for regolith generation and mobility at the Susquehanna Shale Hills Critical Zone Observatory, PA

From Microns to Mountains: Using diffusion models to measure reaction rates in metamorphic rocks

Alicia Cruz-Uribe
Ph.D. Student, Pre-comps

Advisor: Maureen Feineman

Determining the timescales over which metamorphic reactions occur has long been an important and difficult question to answer. Recent work has found many orders of magnitude difference between slow regional (dry) rates and fast contact metamorphic (hot and wet) rates; subduction zone metamorphism is expected to fall somewhere in between. Here we examine rutile replacement by titanite in a migmatized garnet amphibolite from Catalina Island, CA and amphibolitized eclogite from Tromsø, Norway. We present two models of Nb back-diffusion in rutile during the rutile to titanite transition in order to estimate the timescales and rate of reaction.

Trace element concentrations in rutile and titanite were determined by LA-ICP-MS for grains in one sample from Catalina Island. Niobium profiles across two rutile grains (500-700 μm) show clear evidence for Nb back-diffusion into rutile during titanite growth at the grain boundary. The same feature was reported and modeled by Lucassen et al. (2010) for Nb and Zr in a 7 mm rutile from Tromsø, Norway. Zr-in-titanite thermometry suggests temperatures of ~750°C for the Catalina and ~650°C for Tromsø. New experimentally determined diffusion coefficients for Nb in rutile (R. Dohmen, pers. comm.) at these temperatures were used to model Nb back-diffusion in the Catalina rutile, and to revisit the Tromsø sample in light of the new diffusion data.

A simple 1-D fixed boundary diffusion model was used to model Nb and Zr back-diffusion in rutile and gives timescales of $0.2 - 1 \times 10^5$ yrs for Catalina rutile and $1.4 - 6.4 \times 10^7$ yrs for Tromsø rutile. This is equivalent to a rate of $0.8 - 4.6 \times 10^{-5}$ a^{-1} for Catalina and $0.7 - 7 \times 10^{-8}$ a^{-1} for Tromsø. Using a 1-D moving interface model yielded reaction front velocities, which were then converted to time by using the distance the boundary had moved relative to the pre-reaction rutile surface. Reaction rates of $3 - 7 \times 10^{-6}$ a^{-1} were determined using the moving interface model for Catalina and $0.1 - 1 \times 10^{-9}$ a^{-1} for Tromsø, which are within an order of magnitude of those calculated using the fixed boundary model. In order to compare these to other rates in the literature, the reaction rates were normalized to the surface area of the rate-limiting mineral per unit of rock (R_{net}, $g/cm^2/a$). Normalized reaction rates for Catalina are $2.6 - 6.5 \times 10^{-6}$ $g/cm^2/a$ and for Tromsø are $0.2 - 2 \times 10^{-8}$ $g/cm^2/a$, which suggests 2-3 orders of magnitude difference in R_{net} over ~100°C change in temperature for the rutile-titanite reaction. The values for Tromsø are similar to those determined for regional metamorphic settings, whereas those for Catalina are about 2 orders of magnitude faster, which is consistent with a migmatitic subduction setting with more heat and fluid than a regional setting.

Lucassen et al., 2010, Cont. Min. Pet. 160:279-295.

Geochemical Insights into Multi-component Mantle Beneath the Anatolian Plate

Megan Pickard
Ph.D. Student, Post-comps

Advisor: Tanya Furman

The WSW movement of Anatolia in response to collision between the African/Arabian and Eurasian plate results in complex interaction between compressional and extensional regimes. The subducted slab is seen with tomographic data to be torn beneath Central Anatolia (Biryol et al. 2009) and undergoing rollback in Western Anatolia (Le Pichon & Angelier 1981, Bozkurt 2001); seismic data indicate that beneath Eastern Anatolia portions of the slab have detached entirely (Zor 2008). The isotopic geochemistry of mafic volcanics in each area provide a window into the asthenosphere across the region, enabling determination of both mantle flow patterns and source reservoir compositions. Previous isotopic work uncovered extreme variability both within and between the three major volcanic regions. Our analysis of Sr-Nd-Pb-Hf isotopes and trace element abundance data reveals consistent patterns and processes that vary in detail over space and time. Ternary variations among Pb isotopic values document an ordered mixing process between "C"-like mantle and a hybrid combination of depleted mantle with an enriched source. The oldest volcanics (Early-Mid Miocene in Western Anatolia, Late Cretaceous-Eocene in Central Anatolia) require the greatest contribution from the enriched source. Post-Miocene basalts from Central and Eastern Anatolia contain a modest contribution from the enriched endmember, whereas post-Late Miocene lavas from Western Anatolia are essentially binary mixtures between depleted mantle and "C". Within Central Anatolia, consistent Nd-Hf-Pb isotopic variations enable us to distinguish between samples that lie on the multi-element mantle array and others that plot off the array and are enriched in La-Ce-Nd and Ba-Th-U but depleted in K-Rb, suggesting incorporation of minor sediment and/or metasomatic contributions. These variations occur on a km-scale in the field, requiring intimate juxtaposition of mantle source materials. Our model has broad regional applicability and indicates a common suite of source materials beneath the entire western Mediterranean basin including NE and SW Syria (Krienitz et al. 2009). Further, they indicate consistent source mixing processes taking place over the past ~250 My beneath the volcanic zones of Anatolia and northern Arabia. We suggest that mixing between asthenosphere and lithosphere initiated throughout the region during the Paleotethyan and that the convecting material currently supporting volcanism in Central and Western Anatolia contains only very minor contributions from continental material. The prevalence of "C"-like mantle in this region is likely linked to upwelling along the margins of the African superplume (Sayit et al. 2010). In addition to documenting the modern flow of depleted mantle around subducting slabs, the combined trace element and Sr-Nd-Pb-Hf isotopic compositions of Anatolian mafic lavas help constrain the history of interaction between the African superswell, depleted mantle and the subducting lithosphere.

Constraints on the magma plumbing system of Hekla volcano, Iceland, from geodetic GPS measurements

Halldor Geirsson
Ph.D. Student, Pre-comps

Advisor: Peter LaFemina

Hekla is one of Iceland's most active volcanoes with 18 documented eruptions for the last 1100 years. It erupted last in 2000, and before that in 1991, 1980-1981, and 1971 although these recent eruptions have been smaller (around 5 times smaller in volume) in comparison with earlier Hekla eruptions which were also spaced farther apart in time. Hekla lies in a somewhat complicated tectonic setting. It is at the intersection of a transform fault zone and a propagating rift zone and thus the displacement field in the area is affected by earthquake sequences and gradual shearing in the transform zones and spreading in the rift zone.

Hekla is an unusual volcano in the sense that it is nearly completely aseismic between eruptions although geodetic measurements show steady deformation. Small earthquakes nucleate only around 90 minutes before eruptions (the 2000 eruption), giving a short timespan for eruption warnings. Accordingly, it has been suggested that Hekla does not have a shallow magma chamber, and in fact modeling of satellite radar interferometry (InSAR) data suggests that Hekla's magma chamber lies at a depth of approximately 14-17 km below the surface (Ofeigsson et al., 2011). In addition, the InSAR data show a subsidence local to the center of the volcano, which has been interpreted as due to loading of the crust from the weight of the volcano itself (Grapenthin et al., 2010). Hence the vertical deformation field is "doughnut shaped" because uplift is observed at a near-circular pattern around the volcano, and subsidence at the center.

For this study we use continuous and episodic GPS data from 1996 to 2010 to investigate further the sources of deformation at Hekla volcano. The GPS data complement the InSAR data because the GPS measurements give the full three-component displacement vector whereas the satellite data only records the surface deformation in the near-vertical line of sight to the satellite. The horizontal GPS velocities show spreading of more than 8 mm/yr across the volcano, in the direction of the plate spreading. Less deflection in GPS velocities is seen along the plate boundary, indicating a more elongated magma chamber along the plate boundary and/or that significant plate spreading is taking place across Hekla.

Grapenthin, R., B.G. Ófeigsson, F. Sigmundsson, E. Sturkell and A. Hooper 2010. Pressure sources versus surface loads: Analyzing volcano deformation signal composition with an application to Hekla volcano, Iceland. *Geophys. Res. Lett.,* 37, L20310.

Ofeigsson, B.G., F. Sigmundsson, A. Hooper and E. Sturkell 2011. InSAR time series analysis at Hekla volcano, Iceland: Inflation periods and crustal deformation associated with the 2000 eruption. *J. Geophys.Res.* in press, doi:10.1029/2010JB007576.

Insights into the Tectonic Development of the Klamath Mountains Province from Thermal Data and Modeling

Rachel Piotraschke
M.S. Student

Advisor: Kevin Furlong

The Klamath Mountains Province (KMP) of northern California and southern Oregon straddles a fundamental transition along the North American plate boundary from subduction to translation; its Neogene to recent tectonic history may therefore provide a window into the evolution of the plate boundary as it undergoes this transition. The Klamath province hosts some of the highest topography along the convergent boundary (Cascadia), but when this topography developed is not clear, and thus whether its development is linked to modern plate boundary processes is unknown. Additionally, this poorly understood uplift history is accompanied by extensional faulting—consisting of both a system of low-angle faults that makes up a regional detachment, and steeper graben-bounding faults—that overprints the eastern part of the KMP at a high angle to the accretionary fabric of the region. These faults appear to have played a significant role in the tectonic development of the KMP, but the specific relationship between this extension and the development of high topography is unknown.

New apatite (U-Th)/He ages from the lower plate of the aforementioned La Grange Detachment (LGD) show a strong trend of younging toward the upper plate of the detachment, confirming and extending a trend seen in earlier data (Batt et al., 2010) and implying that tectonic exhumation along the LGD played a primary role in the cooling history of these samples. The ages indicate that the LGD was active from ~40-20 Ma, with the upper plate being removed at a horizontal displacement rate of ~2-3 km/Myr. The interpretation of the (U-Th)/He ages as representing removal of the upper plate along the detachment also limits total post-detachment erosional exhumation of the lower plate to <2.5 km, or an average rate of less than ~0.15 mm/yr, implying that relatively rapid modern erosion rates must be balanced by a preceding period of low relief and slow erosion, and the modern topography of the Klamath province is a relatively recent development. Additionally, vitrinite reflectance analysis of coal samples distal from the detachment as well as from its upper plate indicate only moderate burial/exhumation since deposition, which is consistent with our hypothesis that the LGD has been the primary driver of exhumation in the eastern KMP since the Eocene.

G. Batt, S. Cashman, J. Garver, J. Bigelow, Am. J. Sci. 310(4) (2010) 261.

Insights into the frictional and hydrologic behavior of the Alpine Fault, West Coast, South Island, New Zealand

Brett M. Carpenter
Ph.D. Student, Post-comps

Advisors: Chris Marone and Demian Saffer

Carolyn Boulton, University of Canterbury, NZ

The Alpine Fault is the major structure accommodating Australia - Pacific plate motion in New Zealand's South Island. The fault, along the west coast of the South Island, is thought to rupture every 200 – 400 years in magnitude (~ 7.9) earthquakes. The dextral-reverse nature of the fault produces earthquakes with up to 10 m of horizontal displacement and several m of vertical displacement. Here we report on laboratory experiments designed to investigate the frictional and hydrologic behavior of the Alpine Fault. In addition, we summarize a recent drilling expedition performed to core and instrument the Alpine fault on the South Island.

We conducted experiments on outcrop samples from two traces of the Alpine Fault, one active (Gaunt Creek (GC) – site of DFDP Holes 1 A/B) and one abandoned (Waikukupa Thrust (WT)). We sheared intact wafers of hanging wall (HW) and principle slip surface (PSS) in a double-direct shear configuration subject to true-triaxial loading under constant effective normal stress, confining pressure, and pore pressure. We report on the frictional behavior (strength, healing, and rate dependence) of these materials at an effective normal stress of 30 MPa. We also report on permeability measurements made on intact wafers of our sample material.

Initial results from experiments show that: 1) the PSS is weaker than the HW samples but has friction of ~ 0.40, 2) both HW and PSS from Gaunt Creek exhibit velocity weakening friction behavior, a condition necessary for fault rupture and earthquake nucleation, and 3) a 5-6 order of magnitude permeability difference between PSS and HW at both WT and GC. Our permeability data, combined with geophysical logging (33m head difference across the fault) and observations of gouge injection features, indicates that the PSS of the Alpine Fault becomes pressurized during large slip events, reducing the strength of the fault and allowing rupture to propagate.

Quantifying pressure solution and lithification: tying elastic moduli measurements to changes in porosity and deformation style in sheared granular aggregates

Bryan Kaproth
Ph.D. Student, Post-comps, Petroleum related

Advisor: Chris Marone

Recent studies highlight the role of pressure solution on frictional strength and poromechanical behavior of sheared granular aggregates. In particular, changes in lithification state can affect elastic properties, rheology, and frictional stability of fault rocks. Previously, lithification has been assessed primarily through porosity and microstructure analysis. During experiments where pressure solution is active, we quantify lithification via detailed dynamic bulk and shear modulus measurements, and we relate these measurements to porosity and microstructural observations.

We sheared layers of rock salt in a biaxial loading apparatus under P-T conditions of pressure solution. PZT's were used to actively monitor P- and S-wave velocity continuously as a function of load, shear, and hold time. Our tests include detailed assessment of elastic moduli, strength, porosity, and density. Layers were sheared under saturated and dry (<6% RH) conditions at a given strain rate, and in slide-hold-slide tests. Hold periods ranged from 0- 10,000 s, after which the sample's microstructures were characterized with SEM imaging. During saturated experiments, where pressure solution is dominant, we find that the dynamic bulk and shear modulus increase with hold time, at rates of 1.80 GPa and, although complicated, 0.98 GPa per decade in time, respectively. Increases in the elastic moduli result from stiffness increase of the bulk granular aggregate, related to porosity loss, increased real area of contact, and increased quality of contacts. This evolution affects how the sample deforms with shear. In particular, microstructure analysis shows that the sample experiences enhanced localization, compared to samples where pressure solution was limited. With shear following the hold, saturated samples show porosity increase (from 0.91 to 5.28 %), bulk modulus decrease (42.5 to 36.7 GPa), shear modulus decrease (18.6 to 17.0 GPa), and Vp/Vs ratio decrease (1.51 to 1.46). Enhanced localization, such as observed here, may influence the frictional stability of fault gouge, and could play an important role in seismicity at subduction-zone megathrust faults.

Exhumational and incisional response to active faulting in the Japanese forearc, northeast Honshu

Christine Regalla
Ph.D. Student, Pre-comps

Advisors: Donald Fisher and Eric Kirby

Kevin Furlong, Penn State University
Paul Bierman, University of Vermont

Late Neogene shortening in northern Honshu, Japan is documented along a network of reverse faults and fault-related folds that record Pliocene contractional deformation associated with inversion of Miocene extensional basins. Active slip along several of these structures is recorded by offset Holocene deposits and the presence of topographic scarps, but anthropogenic disturbance of young deposits, deep weathering of the substrate, and thick vegetative cover in the region obscure records of Quaternary slip in many locations. However, the erosional response of fluvial systems to active slip provides a complimentary data set to assess long-term rates and patterns of deformation. Here we present new results from ^{10}Be basin-averaged erosion rates, low-temperature thermochronology, and stream profile analyses within the hanging wall of the Futaba fault in the forearc of northeastern Honshu, that indicate a recent pulse of transient incision and erosion induced by active slip along this thrust fault.

The Futaba fault is a steep, west-dipping reverse fault that bounds the basement-cored Abukuma massif on the east. Tephras in growth strata bracket the initiation of slip along the fault to ~3.9 - 5.6 Ma and yield uplift rates of 0.3-0.5 mm/yr at the southern portion of the fault. This uplift has imparted a topographic signature in the hanging wall of the massif, whose highest elevations are characterized by a low-relief surface with saprolitic bedrock and low-gradient streams. Near the mountain front however, relief and hillslope angles increase, and the surface is deeply dissected by incised bedrock streams. Knickzones in hanging wall streams cluster at ~400m elevation, and are located coincident with this topographic transition. Basin-averaged ^{10}Be erosion rates from catchments above these knickzones are lower than erosion rates below the knickzones by 20-40%. These data are consistent with the upstream migration of knickzones in response to an increase in uplift rate caused by slip along the Futaba fault, but suggest that the geomorphic response to uplift is not adjusted to match Plio-Quaternary uplift rates. AFT ages from hanging wall granites yield ages approximately equal to that of granite emplacement, requiring that the granites have experienced less than 1.8-2.6 km net exhumation in the Cenozoic. These data are consistent with our tectonic model of Mio-Pliocene thrust inversion of a normal fault, and suggest that the morphology observed in the hanging wall of the Futaba fault results from a transient wave of incision imparted by active shortening in the forearc.

Using meteoric ^{10}Be as a tracer for regolith generation and mobility at the Susquehanna Shale Hills Critical Zone Observatory, PA

Nicole West
Ph.D. Student, Pre-comps

Advisor: Eric Kirby

Paul Bierman, University of Vermont

We present preliminary analysis of meteoric ^{10}Be measurements from 30 hillslope soil and bedrock core samples collected from the Susquehanna Shale Hills Observatory (SSHO). The SSHO is located in central Pennsylvania and comprises an E-W trending, first-order watershed developed entirely on Silurian-aged shale. Two major perturbations to the landscape have occurred at SSHO in the geologically recent past, including sustained periglacial activity until after the retreat of the Laurentide ice sheet (~21 ka) and deforestation during early colonial land-use. We measured meteoric ^{10}Be concentrations in bulk soil samples (n=16) collected along a north-facing, planar hillslope, representing ridge top (RT), mid-slope (MS) and valley floor (VF) positions. Our measurements were co-located with analyses of elemental concentrations and U-series disequilibrium estimates of weathering duration. In addition, rock chip samples (n=14) were analyzed from a 24 m deep core drilled into the northern ridge top.

All meteoric ^{10}Be concentration profiles show a declining trend with depth, with most of the ^{10}Be retained in the upper-most decimeters of the soil. Meteoric ^{10}Be inventories are higher at the MS and VF sample sites, at 3.71 ± 0.02 x 10^{10} at/cm^2 and 3.69 ± 0.02 x 10^{10} at/cm^2, than at the RT site (1.90 ± 0.01 x 10^{10} at/cm^2). Meteoric ^{10}Be concentrations are an order of magnitude lower in rock at the DC-1 site than in hillslope soils, ranging from 1.7 x 10^{8} at/g at the surface to 1.3 x 10^{6} at/g at depth. Our data suggest that the majority of delivered meteoric ^{10}Be is retained in the soil cover and does not penetrate deep into bedrock. The ^{10}Be inventory at the convex RT site implies a minimum soil residence time of 10.6 ka, or if erosion is steady, an erosion rate of 19.4 ± 0.2 m/My. These data are within error of those estimated using U-series disequilibrium and are well within the nominal range of erosion rates reported for the Appalachians using *in situ* produced ^{10}Be at 17 ± 9 m/My. Our results provide preliminary data toward understanding the rate and timing of soil formation and transport at SSHO as a function of geologically recent climatic and anthropogenic perturbations.

Oral Session Three A:
Ice and Climate

Saturday, March 19
1:15-2:45 pm, 114 EES

Time	Presenter	Advisor	Title
1:15	Knut Christianson	Sridhar Anandakrishnan	Subglacial Water System of Whillans Ice Stream, West Antarctica
1:30	Lucas Zoet	Sridhar Anandakrishnan	Field and Laboratory Observations Displaying Regularly Repeating Ruptures Beneath Glaciers
1:45	Karen Smith	Christopher House	Exploring the Fate of Nitrogen Heterocycles in Complex Prebiotic Mixtures
2:00	April Roberson	James Kasting	A Laughing Gas Greenhouse for the Proterozoic?
2:15	Ying Cui	Lee Kump	Modern rates of fossil-fuel burning exceed rates of fossil carbon emission during the Paleocene-Eocene Thermal Maximum
2:30	John Fegyveresi	Richard B. Alley	Investigating seasonal influences on firn characteristics, stratigraphic layering, bubble trapping, and climate proxy data at the WAIS Divide site, West Antarctica

Subglacial Water System of Whillans Ice Stream, West Antarctica

Knut Christianson
Ph.D. Student, Post-comps

Advisor: Sridhar Anandakrishnan

Robert Jacobel, St. Olaf College
Huw Horgan, Victoria University of Wellington
Sridhar Anandakrishnan, Penn State University

Recent satellite laser altimetry observations have revealed numerous ephemeral elevation anomalies on West Antarctic ice streams. These anomalies have been interpreted as the surface manifestation of a dynamic subglacial water system where a positive elevation anomaly (on the order of several meters) is due to the filling of a dynamic subglacial lake which subsequently drains over a period of several months. For any given elevation anomaly, these filling/draining cycles repeat over the timescale of a few years and each cycle drains several cubic kilometers of water/sediment either down-glacier or directly to the ocean. The relatively short time-scale of subglacial water/sediment transport compared to other drivers glacial flow variability, proximity of dynamic subglacial lakes to both the onset of streaming flow on ice streams and grounding-lines along West Antarctica's Siple Coast, and volume of sediment and water transported suggest a mechanism for rapid changes in ice stream dynamics. Here we use a variety of geophysical techniques to present both a synoptic scale view of the subglacial water system under Whillans Ice Stream and also a site survey of a specific subglacial lake, and discuss their role in the changing dynamics of Whillans Ice Stream.

Field and Laboratory Observations Displaying Regularly Repeating Ruptures Beneath Glaciers

Lucas Zoet
Ph.D. Student, Pre-comps

Advisor: Sridhar Anandakrishnan

Richard B. Alley, Pennsylvania State University
Chris Marone, Pennsylvania State University

We report on a pattern of repeating earthquakes associated with the flow of David Glacier through the Transantarctic Mountains. These events illuminate processes associated with slip of ice and more generally, stick-slip behavior of earthquake faults. We used data from the Transantarctic Mountain Seismic Experiment (TAMSEIS) network as well as GSN (Global Seismic Network) stations to examine the seismicity of the region in the period 2000-2010. The seismic events recurred regularly (approximately 20 minutes) for a 275-day span in 2001 and 2002. Before and after this 275-day period, the recurrence was more irregular. Source-location measurements determined that the events originated from the base of David Glacier. Analysis of P-wave first-motions indicate that the events are low-angle thrust faults with a fault-strike normal to the flow of David Glacier and a fault slip along flow. The events are of mean magnitude Mw=1.8 and are likely caused by an asperity beneath David Glacier that regularly releases stress accumulated by the flow of the glacier. We suggest that the change in seismic behavior is due to changes in debris concentration of the basal ice over time. The variation of debris load in contact with the asperity produces deformational alterations of the ice asperity system, resulting in the observed behavior.

In order to study how changes in entrained debris affects deformation of ice; we froze a number of ice samples with varying amounts of debris between 1-60% by weight. These samples of ice were sheared in a single direct shear apparatus against a piece of Westerly granite at velocities ranging from 3 to 300 microns per second under a normal load of 1.25 MPa. Frictional values were recorded for each sample of ice. Slide-hold-slide experiments were conducted, which report that an increase in hold time increased the strength of the ice, indicating healing was taking place. Velocity stepping tests were conducted showing a transition from a velocity strengthening to a velocity weakening material near a velocity of 10 microns per second. The transition had secondary effects imposed from the amount of debris contained within. We suggest that this measurement is compatible with our observations of the slipping behavior of David Glacier. Next, the stiffness of the shearing apparatus was reduced using springs to allow stick-slip behavior to occur at the low normal stresses (500 kPa) and shear stresses (150 kPa) that were used in the experiment. We successfully produced stick-slip behavior in the lab. Similarities between laboratory results and field observations are beginning to emerge which will help to scale from the one to the other.

Exploring the Fate of Nitrogen Heterocycles in Complex Prebiotic Mixtures

Karen E. Smith
Ph.D. Student, Pre-comps

Advisor: Christopher H. House

Michael P. Callahan, NASA Goddard Space Flight Center
Henderson J. Cleaves, The Carnegie Institution for Science
Jason P. Dworkin, NASA Goddard Space Flight Center

A long-standing question in the field of prebiotic chemistry is the origin of the genetic macromolecules DNA and RNA. DNA and RNA have very complex structures with repeating subunits of nucleotides, which are composed of nucleobases (nitrogen heterocycles) connected to sugar-phosphates. Due to the instability of some nucleobases (*e.g.* cytosine), the difficulty of synthesis and instability of D-ribose, and the likely scarcity of activated phosphates necessary to form nucleotides, it has been proposed that the first genetic material used alternative nucleotides (Joyce *et al.*, 1987). We have begun to investigate the chemistry of nitrogen heterocycles in plausible, complex prebiotic mixtures in an effort to identify robust reactions that might form potential alternative nucleotides.

We have taken a complex prebiotic mixture produced by a spark discharge acting on a gas mixture of N_2, CO_2, CH_4, and H_2 and reacted it with four nitrogen heterocycles: uracil, 5-hydroxymethyluracil, guanine, and isoxanthopterin (2-amino-4,7-dihydroxypteridine). The products of the reaction between the spark mixture and each nitrogen heterocycle were characterized by liquid chromatography coupled to UV spectroscopy and Orbitrap mass spectrometry. We found that the reaction between the spark mixture and isoxanthopterin formed one major product, which was a cyanide adduct. 5-hydroxymethyluracil also reacted with the spark mixture to form a cyanide adduct, uracil-5-acetonitrile, which has been synthesized previously by reacting HCN with 5-hydroxymethyluracil (Robertson and Miller, 1995). Unlike isoxanthopterin, the chromatogram of the 5-hydroxymethyluracil reaction was much more complex with multiple products including spark-modified dimers. Additionally, we observed that 5-hydroxymethyluracil readily self-polymerizes in solution to a variety of oligomers consistent with those suggested by Cleaves (2001). Guanine and uracil, the biological nucleobases, did not react with the spark mixture, even at high temperature (100 °C). This suggests that there are alternative nucleobases that are more reactive under prebiotic conditions and may have been involved in producing precursor nucleotides.

Cleaves (2001) Diss. University of California, San Diego.
Joyce, Schwartz, Miller, and Orgel (1987) *Proc. Natl. Acad. Sci.*, 84: 4398-4402.
Robertson and Miller (1995) *Science,* 268: 702-705.

A Laughing Gas Greenhouse for the Proterozoic?

April Lynne Roberson
M.S. Student

Advisor: James F. Kasting

Janis Roadt, Department of Physics and Astronomy, University of Wisconsin-Eau Claire
Itay Halevy, Department of Geological and Planetary Sciences, Caltech

An anoxic, sulfidic ocean that may have existed during the Proterozoic Eon (0.54-2.4 Ga) would have had limited trace metal abundances because of the low solubility of metal sulfides., The lack of copper, in particular, could have had a significant impact on marine denitrification. Copper is needed for the enzyme that controls the final step of denitrification, from N_2O to N_2. Today, only about 5-6 percent of denitrification results in release of N_2O. If all denitrification stopped at N_2O during the Proterozoic, the N_2O flux could have been 15-20 times higher than today, producing N_2O concentrations of several ppmv. CH_4 concentrations may also have been elevated during this time, as has been previously suggested. A lack of dissolved O_2 and sulfate in the deep ocean should have produced a high methane flux from marine sediments, as much as 10-20 times today's methane flux from land. The photochemical lifetime of CH_4 increases as more CH_4 is added to the atmosphere, so CH_4 concentrations of up to 100 ppmv are possible during this time. The combined greenhouse effect of CH_4 and N_2O could have provided ~10 degrees of warming, thereby keeping the surface warm during the Proterozoic without necessitating high CO_2 levels. A second oxygenation event near the end of the Proterozoic would have resulted in a reductions of both atmospheric N_2O and CH_4, perhaps triggering the Neoproterozoic "Snowball Earth" glaciations.

Modern rates of fossil-fuel burning exceed rates of fossil carbon emission during the Paleocene-Eocene Thermal Maximum

Ying Cui
Ph.D. Student, Pre-comps

Advisor: Lee Kump

The Paleocene-Eocene Thermal Maximum has been proposed as an ancient analogue for future climate response to CO_2 emission from fossil fuel burning. However, the source, rate, and total amount of C input to the ocean and atmosphere at the time remain poorly known. Here we present isotopic and geochemical data from a highly expanded marine sedimentary section in Spitsbergen that provides an exceptional level of temporal resolution and completeness of the carbon isotopic excursion recorded in organic matter deposited during the PETM. Total organic C $\delta^{13}C$ values constrain the magnitude of the carbon isotope excursion in the ocean-atmosphere system to ~ 4‰. We force an earth system model of intermediate complexity (EMIC) to conform to the isotope record, and thereby determine a continuous estimate of variations in the rate of carbon addition. We find that despite uncertainty in the isotopic composition of the source and the duration of the event, the peak rate of C addition was likely much slower (0.3-1.7 Pg C/yr) than the current fossil fuel burning rate[1] (9 Pg/yr).

1.   Le Quéré, C., Raupach, M.R., Canadell, J.G., Marland, G. & et al. Trends in the sources and sinks of carbon dioxide. *Nature geoscience* **2**, 831-836 (2009).

Investigating seasonal influences on firn characteristics, stratigraphic layering, bubble trapping, and climate proxy data at the WAIS Divide site, West Antarctica

John M. Fegyveresi
Ph.D. Student, Pre-Comps

Advisor: Richard B. Alley

Knowledge of climate history is of value in understanding and attributing climate change. Ice cores are remarkably valuable in providing information on crucial variables of climate history by supplementing and extending instrumental data. A better understanding of the processes by which firn (old snow) turns to ice, will not only yield more robust data sets and possible new measurement techniques, but can also help to identify the potential for biasing in ice-core proxy data. Diurnal and seasonal variations, as well as the timing of accumulation in polar regions, affects the near-surface firn through changes in the exposure to various meteorological, atmospheric, and turbulent fluxes. These changes can result in greater surface metamorphism, evaporation, sublimation, convection in the snow pack, surface crusting, and more pronounced grain growth. At sites with higher overall accumulation rates and frequency of individual depositional events, like WAIS Divide, this can result in highly layered, irregularly-stratified firn with numerous internal features and high density contrast. If preserved at depth, this high degree of layering and internal features may impart a bias on the process of bubble trapping at pore close-off and result in falsely interpreted climate variability in ice-core proxy data. Here we are investigating recently obtained bubble number-density, total gas content, high-resolution chemistry, and crystal size and orientation data from the WDC06A ice core, in order to discern evidence of these possible seasonal biases. Additionally, real-time snowpit, surface, meteorological and net-solar energy data from three concurrent field seasons are being analyzed in order to better quantify the conditions and net-surface energy flux surrounding near-surface metamorphism. Specifically, we are investigating the formation of distinct and pronounced surface crusts, or "glazes", observed at the site. These noteworthy features, and the processes which lead to their formation, are not yet well understood at high-accumulation rate sites like WAIS Divide. Assuming a Nye-thinning model, the preservation of these crusts at depth could affect various proxy data.

Oral Session Three B:
Isotope geochemistry and Hydrogeology

Saturday, March 19
1:15-2:45 pm, 116 EES

Time	Presenter	Advisor	Title
1:15	Piyali Chanda	Matthew Fantle	Strontium Isotopic Constraints for the Age of Eocene Marine Mammal Horizon of Kutch, Western India
1:30	Khadouja Harouaka	Matthew Fantle	Investigation of Calcium Isotopic Fractionation in Gypsum
1:45	Heather Tollerud	Matthew Fantle	Mapping playa surfaces in dust-producing regions: Extending geochemical measurements over large scales with remote sensing
2:00	Emily Comer	Rudy Slingerland	Depositional Environments of Late Danian Plant Localities: Chubut Province, Patagonia
2:15	Julianne Hagarty	Kamini Singha	Land Use, Water Quality, and Incidence of Buruli Ulcer in Gold-Mining Regions of Ghana
2:30	Ryan Swanson	Kamini Singha	Anomalous Transport in Groundwater

Strontium Isotopic Constraints for the Age of Eocene Marine Mammal Horizon of Kutch,Western india

Piyali Chanda
Ph.D. Student, Pre-Comps

Advisor: Dr. Matthew S. Fantle

The primary objective of this study was to determine numerical age of a middle Eocene marine horizon of Kutch, Western India using isotopic composition of Strontium in carbonate. The age of this horizon is poorly constrained because of absence of age diagnostic fossils. Now, middle Eocene marine mammal faunas, especially whales (Cetacea) and sea-cow (Sirenia), are long-known to occur in the Tertiary succession of Kutch, especially in the Harudi Formation of Kutch. Of the cetaceans, remingtonocetids are particularly abundant and diverse and represents one of the primitive stages in the evolutionary transition of whales from land to sea. Therefore, it becomes very important to determine the precise age of this vertebrate-yielding horizon in order to contribute to our understanding of the evolutionary history and global correlation of whales and associated marine mammals of South Asia to the other whale-bearing strata.

The age of the whale- bearing strata in Kutch is poorly resolved, with opinion divided between Lutetian and Bartonian stages of the middle Eocene. In conjunction with the biostratigraphy, Strontium Isotope Stratigraphy is a useful tool to determine the numerical age of the marine sedimentary horizons precisely. In SIS, the strontium isotopic ratio ($^{87}Sr/^{86}Sr$) of marine carbonates (both sediments and skeletal remains of marine fauna) is determined. Although this method is mainly useful for the strata of Oligocene and younger ages, with the aid of advanced instruments and better precision, it has now become applicable for the older strata (such as Eocene, Paleocene, Cretaceous). Here an attempt has been made to determine the precise numerical age of marine mammal-bearing horizon of Tertiary succession of Kutch, Gujarat, analyzing the strontium isotopic ($^{87}Sr/^{86}Sr$) composition of selected samples of oysters and other marine forms (mollusks and foraminifers) reported from this horizon. The age of the Harudi Formation, the whale-bearing horizon of Kutch, obtained from the palaeontological data, is widely considered to be Middle Eocene. Since middle Eocene encompasses a wide age range, starting from 49.0 Ma to 37.0 Ma, it becomes difficult to pinpoint the specific numerical age of Harudi Formation. Based on the standard look-up tables for strontium isotope ratios (LOWESS curve), two clusters of numerical ages (~ 47 Ma and ~ 42 Ma) have been obtained in this study.

Investigation of Calcium Isotopic Fractionation in Gypsum

Khadouja Harouaka
M.S. Student

Advisor: Matthew Fantle

A series of gypsum growth experiments were carried out using stock solutions of $CaCl_2.2H_2O$ and Na_2SO_4. Gypsum growth rates were determined as a function of varying saturation state, ionic strength and calcium to sulfate ratio. Solutions with initial saturation state of 3.6 and initial ionic strength of 0.5 produced white micro crystals at rates ranging from $6.7x10^{-6}$ to $3.5x10^{-6}$ $Mm^{-2}s^{-1}$. Solutions with calcium to sulfate ratio of 1.5 produced crystals at a faster rate than solutions with ratio of 0.7. BET surface area analysis of these crystals ranged from 2.0 to 0.8 m^2g^{-1}. SEM images indicated flat euhedral crystals around 10 to 20 microns in length and width. Solutions with initial saturation state of 1.8 and initial ionic strength adjusted to 0.5 by the addition of 5M NaCl produced a very poor yield of crystals at rates estimated to range from $7x10^{-8}$ to $3x10^{-8}$ Ms^{-1}. These experiments yielded too few crystals for BET surface area analysis, but SEM images of the residue from the filtered solutions showed needle like crystals of around 100 to 300 microns in length. Reducing the ionic strength of these growth solutions to 0.2 resulted in a greater yield of similarly sized crystals and an increase of rate to around $2x10^{-7}$ $Mm^{-2}s^{-1}$. The results of these experiments demonstrate the dependence of crystal growth rate on various chemical properties of the growth solution which are likely to be reflected in $\delta^{44}Ca$ values of the crystals. This may also explain inconsistencies in calcium isotopic fractionation patterns discerned from calcite precipitation experiments (Lemarchand et. al, 2004; Tang et. al, 2008).

Lemarchand D., Wasserburg G., Papanastassiou D.; Rate-controlled calcium isotope fractionation in synthetic calcite; *Geochimica et Cosmochimica Acta* **2004**; 68 4665-4678

Tang J., Dietzel M., Bohm F., Kohler S., Eisenhauer A.;Sr^{2+}/Ca^{2+} and $^{44}Ca/^{40}Ca$ fractionation during inorganic calcite formation: II. Ca isotopes; *Geochimica et Cosmochimica Acta* **2008**; 72 3733-374

Mapping playa surfaces in dust-producing regions: Extending geochemical measurements over large scales with remote sensing

Heather Tollerud
Ph.D. Student, Pre-comps

Advisor: Matthew Fantle

Elmore, A. J, University of Maryland Center for Environmental Science

Mineral dust is an important component of geochemical cycles, but its impact on those cycles is not thoroughly understood. The impact of dust on geochemical cycles is determined by the chemical and mineralogical composition of dust inputs, which is governed in turn by the composition of the dust source region. A loose, unconsolidated surface texture is more easily ablated by wind, and so a location where composition and environmental characteristics encourage this type of surface is more likely to produce dust and influence geochemical cycles. Also, if evaporites (such as calcite) are concentrated at the surface of a dust producing region through evaporation, dust Ca concentrations are likely to be higher than would be expected based on the composition of the surrounding bedrock. Playas can be regionally significant dust source regions, and they are amenable to study as their surface textures often vary significantly across small areas and can change over time. This study investigates the elemental geochemistry of surface sediments and surface structure in a large playa system (Black Rock Desert) in northwestern Nevada (USA). We collected approximately 50 samples and their spectra from the Black Rock Desert in July/August 2007. From x-ray diffraction and ICP-OES, we found that calcite concentrations in the samples range from 5 to 15 wt.%. We used these values to evaluate a map of calcite content based on a spectral feature in satellite hyperspectral data from the Hyperion instrument. In this map, calcite is less common near the center of the playa, which is more frequently under water. Additionally, the mineral content of playa surfaces may be useful as an indicator of processes responsible for generating variations in surface texture, in particular the precipitation of evaporite minerals related to the movement of water. We examined two years of radar data from the ENVISAT Advanced Synthetic Aperture Radar instrument as a proxy for surface texture, and found that the distribution of surface structures changes significantly between summers, especially near the center of the playa. By elucidating some of the connections between the physical and chemical properties of playa sediments, this work serves as a foundation to predict the effects of changing climatic conditions on dust and to extend observations of modern systems to the geologic past and future.

Depositional Environments of Late Danian Plant Localities: Chubut Province, Patagonia, Argentina

Emily Comer
M.S. Student

Advisor: Rudy Slingerland

Peter Wilf, Penn State University

Diverse, well-preserved macroflora are observed within Cretaceous and Paleocene sediments of Chubut Province, Patagonia, Argentina. Two important sites of fossil preservation, Palacio de los Loros and Parque Provincial Ormachea, sit near the top of the Late Danian (65.5-61.7 Ma) Salamanca Formation. Understanding the depositional history of the Salamanca is important in characterizing paleoenvironments in which these flora lived and relating these Patagonian macroflora to concurrent Paleocene flora within the Gondwanan supercontinent. During a two week field season, thirteen stratigraphic sections were measured along the outcrop belt at Palacio de los Loros and Ormachea Park as well as two minor sites; Las Flores, and Rancho Grande. Photo mosaics, laser ranger data, and stratigraphic columns were merged with elevated geologic maps and imported into Fledermaus to generate a 3-D visualization of facies relationships. Rock samples were collected, thin sectioned and analyzed for petrography and grain size. The Salamanca Fm. in the study region consists of seven dominant facies: 1) transgressive sands, 2) wispy-bedded clays, 3) flaser bedded silts, 4) heterolithic cross-bedded sands, 5) white cross-bedded sands, 6) accretion-bedded silts, and 7) transitional silty clays. The base of the Salamanca Fm. rests on an unconformity representing the gap between Cretaceous and late Danian sediments defining both a sequence boundary and marine flooding surface. Lower sections of the Salamanca contain abundant glauconite and fossils characteristic of a marine shelf environment. These facies transition upwards to bi-directional trough cross-bedded sands interspersed with flaser bedded sandy silts indicative of meso-tidal currents with dominant orientations of ESE (340-360 degrees) and SW (240 degrees). The uppermost unit of the Salamanca Fm. gradationally transitions to silts containing abundant, well-preserved compression macrofloras representative of a diverse lowland forest. Overlying the Salamanca Fm. are black muds in the Banco Negro Inferior of the Rio Chico Formation, interpreted as a series of stacked gleyed paleosols in a widespread continental swamp and indicating a gradual progradation of the estuary. Two-dimensional hydrodynamic modeling of tidal currents and ranges in the proto-San Jorge embayment produce wave amplitudes of 1-2 meters, consistent with the hypothesis that the Salamanca Fm. was deposited in an open estuary that amplified Paleocene Atlantic tides to meso-tidal range. Synthesis of facies relationships, wireline log character, hydraulic modeling, petrography, macrofloras and geochemistry define a detailed Paleocene environment for the Salamanca Fm. in the study area.

Land Use, Water Quality, and Incidence of Buruli Ulcer in Gold-Mining Regions of Ghana

Julianne Hagarty
M.S. Student

Advisor: Kamini Singha

Buruli ulcer, an emerging bacterial disease caused by *Mycobacterium ulcerans*, affects populations in many equatorial countries, predominantly in western Africa. Occurring in over thirty countries worldwide, it is the third most common Mycobacterial disease after tuberculosis and leprosy. The disease causes ulcerative lesions and can lead to severe deformity if untreated. While methods of treatment for Buruli ulcer are well known and have a high rate of success, the mode of transmission of Buruli ulcer remains elusive. Multiple hypotheses have been put forward in the search for the vector for this disease. Studies of Buruli ulcer to date seem to conclude that water is, in some way, closely related to the transmission of this disease. Additionally, changes in water quality due to changes in land use may contribute to the emergence of Buruli ulcer[1]. In my work, I hypothesize that stagnant pools, especially those with low dissolved oxygen and high metals, nitrogen, and phosphorus concentrations, will provide a favorable environment for *M. ulcerans* growth and transmission. I also hypothesize that water quality will be closely coupled to land use.

To explore how climate, human behavior, land use, and soil and water quality interact to create a favorable environment for Buruli ulcer emergence, I present studies of rainfall and temperature, land use, physical and chemical properties of soil and water, and counts of *M. ulcerans* in soil and water. Groundwater data from the Community Water and Sanitation Agency in Ghana were analyzed using cluster and principal components analyses. Initial results indicate that aquifer rock type does not strongly correlate with groundwater chemistry and that groundwater chemistry does not relate to incidence of Buruli ulcer. Analyses of rainfall data collected from eleven stations throughout Ghana show that patterns of annual rainfall do not vary greatly between Buruli-endemic and non-endemic areas, suggesting that normal rainfall patterns do not affect incidence of disease. Analysis of localized soil and water chemistry is ongoing, and I expect that water bodies near mines and farms will be a favorable environment for *M. ulcerans* growth due to some combination of low dissolved oxygen, high metals, and high nitrogen and phosphorus concentrations.

---

[1] Merritt, R.W., Benbow, M.E., Small, P.L.C. (2005). "Unraveling an emerging disease associated with disturbed aquatic environments: the case of Buruli ulcer." *Frontiers in Ecology and the Environment*, **3**, 323-331.

Anomalous Transport in Groundwater

Ryan David Swanson
Ph.D. Student, Pre-comps

Advisor: Kamini Singha

The processes governing groundwater contaminant transport are poorly understood due to an incomplete understanding of mass-transfer. At many field sites, tailing behavior-- a long, slow decrease of concentration in time-- is observed that cannot be explained by the classical advection-dispersion transport equation. Tailing behavior can be explained by exchange between a less-mobile and mobile domain. However, the rate and scale-dependency of mass transfer is poorly understood. Standard fluid samples only measure the mobile phase, while electrical resistivity measurements, a function of the total solutes of both the immobile and mobile domain, are used to observe mass exchange between the two domains. The synthesis of co-located bulk electrical conductivity and fluid conductivity measurements can be used to calculate the mass transfer rate through a temporal-moment analysis. However, measurements of the parameters controlling this exchange have yet to be performed outside of numerical modeling.

Here, we directly measure mass transfer rates at the lab-scale using temporal moments from bulk and fluid conductivity measurements. Column tracer tests are performed on well-sorted sand and the porous zeolite clinoptilolite. The zeolite's internal porous network acts as immobile domain. Using sodium chloride solution as a tracer, tracer experiments are performed on the two media at various flow rates with potential electrodes used for electrical geophysics spaced every 2.5cm on the sides of the columns in addition to current electrodes placed at the top and bottom to measure bulk electrical conductivity. Fluid electrical conductivity is measured with a flow-through conductivity probe at the end of the column. Parametric sweeps are performed in COMSOL Multiphysics by adjusting parameters including the mobile and immobile porosity and the mass transfer rate. The simulation results are compared to the measured fluid conductivity of the mobile domain, and the best-fit parameters are determined by the least root mean square error between the simulations and measurements. Geophysical inversions performed in R3t, a 3-D Occam's type solution code, provide detailed spatial and temporal resolution of tracer movement throughout the column. The mass transfer rates will be determined using temporal moments from the bulk and fluid electrical conductivity measurements and compared to best-fit results from the parametric sweeps.

Oral Session Four:
Geobiology

Saturday, March 19
3:00-4:15 pm, 114 EES

Time	Presenter	Advisor	Title
3:00	Monica Carvalho	Peter Wilf	Ferns from the Laguna del Hunco paleoflora (51.9 Ma), Patagonia, Argentina, reveal new biogeographic links to rainforest Gondwana
3:15	Eriks Perkons	Mark Patzkowsky	The contribution of regional variability to beta diversity: a case study of the deep-water marine communitites of the middle Upper Ordovician of eastern Laurentia
3:30	Travis Deptola	Mark Patzkowsky	Quantifying Faunal Stability Through Time: Biofacies Identification of the Middle Devonian Hamilton Group in Central Pennsylvania
3:45	Lauren Milideo	Russ Graham	An Ecological Gradient in Midwestern North American Late Holocene Localities
4:00	Christen Miller	Peter Wilf	A preliminary pre-settlement flora of White Clay Creek, Chester County, Pennsylvania

Ferns from the Laguna del Hunco paleoflora (51.9 Ma), Patagonia, Argentina, reveal new biogeographic links to rainforest Gondwana

Mónica R Carvalho
M.S. Student

Advisor: Peter Wilf

María A. Gandolfo, L.H. Hortorium, Cornell University
Rubén Cúneo, Museo Paleontológico Egidio Feruglio, Chubut, Argentina
Kirk Johnson, Denver Museum of Nature and Science

The fossil record of Cenozoic ferns in South America is notably scanty, mostly due to the naturally low abundance of ferns in angiosperm-dominated forests, as well as a lack of continuous, systematic sampling on the continent. Likewise, fossil fern identification relies on the uncommon preservation of reproductive structures, leading to a poorly known and uninterpretable biogeography for the South American Cenozoic. We report four fertile fern genera from the Laguna del Hunco paleoflora, a montane rainforest assemblage better known for its extraordinary angiosperm diversity. This flora is preserved in caldera-lake deposits from the early Eocene (51.9 Ma) of Patagonia, Argentina, and has been shown to reflect the floristic connection between South America and Australasia via Antarctica at this time. The genera represent *Todea* (Osmundaceae), *Sticherus* (Gleicheniaceae), *Dicksonia* (Dicksoniaceae) and Pteridaceae (cf. *Adiantum spp.*), identified based on vegetative characteristics and soral or sporangial morphology. These 4 families share deep time divergences as evidenced by a fossil record that extends back into the Late Paleozoic and Mesozoic. *Todea* is now restricted to montane, humid subtropical and tropical Australasia and South Africa, and has been reported from late Cretaceous deposits of British Columbia and the Jurassic of Argentina. *Todea* seems to show a much broader distribution in the past than their extant counterparts, a pattern also seen with most Cenozoic ferns of the northern hemisphere. *Dicksonia* is present in the wet subtropics and tropics of Australasia and South America, and *Sticherus* is pantropical and austral, and mostly humid montane. Their fossil records remain sparse; both genera are known from Oligocene deposits of Tasmania, and *Dicksonia* has been also described from a middle Eocene flora from Argentina. These findings increase the number of tropical elements and more widespread Gondwanan lineages present in Patagonia during the early Eocene, and they support rainforest interpretations. The data contribute to previous biogeographic and rainforest affinities inferred for this paleoflora, which have suggested strongest links to the low latitude West Pacific, with additional connections to the montane neotropics and mid- latitude South America.

The contribution of regional variability to beta diversity: a case study of the deep-water marine communities of the middle Upper Ordovician of eastern Laurentia

Eriks Perkons
M.S. Student

Advisor: Dr. Mark Patzkowsky

The structure and recurrence of marine invertebrate communities along depth gradients has been a recent and productive research subject among paleobiologists studying evolutionary patterns and biostratigraphic correlation. However, the extent to which these communities vary across regional spatial scales has received comparatively little attention. The middle Upper Ordovician Salona and Coburn Formations of the Trenton group carbonates provide an opportunity to quantitatively study faunal community compositions along the deep subtidal to offshore depth gradient. High resolution (5 cm scale) stratigraphic analysis, coupled with extensive fossil collection from several exposures in central Pennsylvania, allows for identification of biofacies and faunal depth preferences. This study locally includes outcrops at Reedsville, Spring Mills, and Lemont from which fossil collections are being assembled, and from which the depositional and environmental history can be assessed.

In addition to providing a greater understanding of local biofacies and geologic history, this study will also compare locally identified biofacies with faunal communities from regional coeval and genetically similar deposits. As the Trenton and Trenton equivalent carbonates were deposited along the long axis of the Taconic foreland basin, they present the opportunity to examine communities over an extensive (ca. 1000 km) stretch of comparable deposits. The presence of widespread K-bentonites allows for precise time correlation of these beds with other regional deposits that share similar depositional histories. Comparison of the faunal communities found in central Pennsylvania with previously reported collections from the Trenton Falls area of New York as well as central Kentucky near Frankfort provides a means of assessing regional variability among equivalent environments, and for investigating the role of different spatial scales in determining beta diversity. The deep subtidal through offshore biofacies have previously been under-sampled, so detailed examination of these strata will provide much needed quantitative community data in addition to insight regarding the primary questions addressed in this study.

Quantifying Faunal Stability Through Time: Biofacies Identification of the Middle Devonian Hamilton Group in Central Pennsylvania

Travis Deptola
M.S. Student

Advisor: Dr. Mark Patzkowsky

In recent years, many paleontological studies of shallow, marine invertebrate communities have attempted to explore the spatial and temporal limits of the theory of coordinated stasis. Since the inception of this theory, several quantitative studies of marine invertebrate fossil assemblages have challenged the ubiquity of the coordinated stasis pattern. Concluding that a geologic interval is experiencing a pattern of taxonomic and ecological "stasis" is a scale-dependent observation, and consequently makes comparisons between studies problematic. Our understanding of the coordinated stasis pattern has been viewed as end-members of a false dichotomy: fossil assemblages are not simply showing "stasis" or "no stasis". A more fruitful avenue of paleoecological research lies in quantifying the varying degrees of stability between fossil assemblages arrayed along different spatial and temporal scales.

The Middle Devonian Hamilton Group of Huntingdon, Pennsylvania is a good candidate for quantifying varying degrees of taxonomic and ecologic stability, and is directly comparable to the time-equivalent Hamilton Group of New York State where the theory of coordinated stasis originated. A high resolution stratigraphic field study incorporating both measured stratigraphic sections and gamma ray logs will constrain the depositional history of the basin, while also ensuring proper chronostratigraphic correlation between sections. Further, the addition of approximately 100 fossil collections provides important, quantifiable paleontological information, including characterization of biofacies, rank abundances of taxa and guild structure, extinction and origination rates, and metrics of diversity. The combination of high resolution stratigraphic measurements and quantifiable metrics of faunal turnover at well-defined spatial and temporal scales provides much needed, comparable data to the field of paleontology. The results of this study will also encourage similar analyses across varying spatial and temporal scales, illuminating broader-scale processes behind faunal turnover dynamics.

An Ecological Gradient in Midwestern North American Late Holocene Localities

Lauren Milideo
Ph.D. Student, Pre-comps

Advisor: Russ Graham

Nonmetric Multidimensional Scaling (NMDS) was employed to examine a late Holocene archaeological/vertebrate paleontological dataset (from the FAUNMAP database, now incorporated in the NEOTOMA database; 1, 2) spanning the Dakotas, Iowa, and Illinois. The sites contain a unique and diverse array of taphonomic histories. Taphonomic factors may act as site filters, often having a large impact on assemblages and resulting analyses. Previous multivariate analysis of a late Holocene Iowa dataset (3) indicates that taphonomic biases may mask the environmental trends of a geographic cross-section of localities.

However, our results suggest that it is possible to obtain a true ecological signal even from heavily taphonomically-influenced data. NMDS and canonical correspondence analysis of this larger dataset indicate that, despite taphonomic differences, the taxa of the sites reflect the environmental gradient from Great Plains to prairie/forest ecotone. We conclude that although taphonomic impacts may be substantial, environmental trends are still detectable with a sufficient number of samples.

1. Graham, R.W., and E.L. Lundelius, Jr. 2010. FAUNMAP II: New data for North America with a temporal extension for the Blancan, Irvingtonian and early Rancholabrean. FAUNMAP II Database, version 1.0. http://www.ucmp.berkeley.edu/faunmap/about/index.html.
2. Graham R, et al. (2009) Neotoma Paleoecology Database, www.neotomadb.org.
3. Semken, Jr. H. and Graham, R.W. 1996. Paleoecologic and taphonomic patterns derived from correspondence analysis of zooarchaeological and paleontological faunal samples, a case study from the North American prairie/forest ecotone. Acta. Zool. Cracov. 39 (1): 477- 490.

A preliminary pre-settlement flora of White Clay Creek, Chester County, Pennsylvania

Christy Miller
M.S. Student

Advisor: Peter Wilf

On America's east coast, the time period immediately surrounding European settlement was characterized by severe and rapid anthropogenic landscape change. Land-clearing for agriculture lead to extensive erosion on hill slopes. The sediment from this erosion and the construction of milldams accumulated behind milldams in valley bottoms. Dam breaching or removal lead streams to incise into the deposited sediment creating meandering streams with raised banks – altering the geomorphology and likely the floristic communities of the region. Despite the magnitude of these changes, few studies have quantified the impact of European colonization on plant communities in the northeastern United States and no known studies have used paleontological data to support their conclusions. Deposited seeds and nuts as well as sedimentological data indicate wetland conditions existed prior to the construction of mill dams, however, these studies provide little evidence of woody riparian species. This study uses leaf subfossils to reconstruct the pre-European settlement flora of White Clay Creek and to test the hypothesis that prior to European settlement wetlands existed in locations in which they are no longer present. Additionally, this study compares the subfossil flora to the modern flora at the site to examine the influence of European settlement on the floral community. Leaf subfossils were collected from a stream cut of the eastern branch of White Clay Creek, processed and identified. Species found at the study site are generally woody species and have a diverse range of wetland affiliations with obligate and facultative wetland species including three morphotypes of willow (*Salix* sp.), Swamp Maple (*Acer rubrum*) and Hazel Alder (*Alnus serrulata*); facultative species including American Beech (*Fagus grandifolia*) and facultative upland species including Scarlet and White Oak (*Quercus coccinea, Q. alba*). The diversity in wetland indicator statuses indicates that leaf subfossils originate both from the riparian buffer and hill slopes. Additionally, the pre-settlement flora contains more wetland species than the modern vegetation supporting the hypothesis that valley bottoms once contained broad wetlands.

Please give us your feedback!

The committee was particularly excited about having the colloquium over a weekend so more people could participate. Please tell us what you thought so we can make it even better next year.

You can remove this page and place it in the comments box at the door of 114 EES or give it to one of the committee members. You can also email Claire Fleeger at crf163@psu.edu.